

Article

# Cross-Shore Modeling Features: Calibration and Impacts of Wave Climate Uncertainties

Frederico Romão <sup>1,\*</sup>, Carlos Coelho <sup>1</sup>, Márcia Lima <sup>1</sup>, Hrólfur Ásmundsson <sup>2</sup> and Eric M. Myer <sup>2</sup>

<sup>1</sup> RISCO & Department of Civil Engineering, University of Aveiro, Campus Universitário de Santiago, 3810-193 Aveiro, Portugal; ccoelho@ua.pt (C.C.); marcia.lima@ua.pt (M.L.)

<sup>2</sup> Vatnaskil, Síðumúli 28, 108 Reykjavík, Iceland; hrolfur@vatnaskil.is (H.Á.); eric@vatnaskil.is (E.M.M.)

\* Correspondence: fredericoromao@ua.pt

**Abstract:** Numerical models can be powerful tools for evaluating the best scenarios for the construction of artificial nourishments to mitigate coastal erosion. Until recent decades, when looking at medium- to long-term simulations, cross-shore and alongshore processes have been studied separately. Accounting for both processes in a shoreline evolution numerical model would improve the understanding and predictive capacity of future changes in coastline evolution. The AX-COAST project aims to develop new capacities in modeling cross-shore sediment transport processes by adding the CS-Model, a cross-shore numerical model, into the existing LTC (Long-Term Configuration) model. The LTC model is a shoreline evolution numerical model which is a module of the cost-benefit assessment tool COAST. This work presents the first steps of the CS-Model implementation, which involve evaluating its performance by calibrating the model with extensive measured datasets of wave climate, beach profiles, tide levels, etc., from coastal areas in IJmuiden and Sand Motor in the Netherlands. The results show good agreement between modeled and observed values. Additionally, wave climate datasets derived from global and regional wave models were considered to evaluate modeling performance at IJmuiden. Using derived timeseries from the wave models did not significantly lead to different results compared to using measured data. The obtained mean absolute and relative errors for each profile were low for both types of datasets. Calibration processes with consistent data are important in modeling simulations to accurately represent the study area and ensure the credibility of future simulations.



**Citation:** Romão, F.; Coelho, C.; Lima, M.; Ásmundsson, H.; Myer, E.M. Cross-Shore Modeling Features: Calibration and Impacts of Wave Climate Uncertainties. *J. Mar. Sci. Eng.* **2024**, *12*, 760. <https://doi.org/10.3390/jmse12050760>

Academic Editor: Rafael J. Bergillos

Received: 26 March 2024

Revised: 16 April 2024

Accepted: 28 April 2024

Published: 30 April 2024



**Copyright:** © 2024 by the authors. Licensee MDPI, Basel, Switzerland. This article is an open access article distributed under the terms and conditions of the Creative Commons Attribution (CC BY) license (<https://creativecommons.org/licenses/by/4.0/>).

## 1. Introduction

In recent decades, artificial nourishments have become one of the main coastal intervention measures to mitigate coastal erosion and climate change effects around the world [1]. This solution is not permanent, and nourishments are usually repeated from time to time depending on their initial design, wave climate, type of sand used and frequency and type of storms [2]. To evaluate the best nourishment intervention scheme, decrease costs and maximize benefits, numerical models can be applied. The AX-COAST project aims to develop new capacities in modeling cross-shore sediment transport processes using a cost-benefit assessment tool, COAST [3]. The COAST tool has three main modules: a shoreline evolution numerical model (Long-Term Configuration model—LTC [4,5]), a coastal intervention pre-design module (XD-COAST [6,7]) and a cost-benefit analysis module.

Medium- to long-term cross-shore and alongshore sediment transport processes have mostly been studied independently [8,9]. Accounting for both cross- and alongshore processes in a shoreline evolution numerical model is relevant to better understand and predict future changes in coastline evolution [10]. Many cross-shore models have been developed in recent decades to study beach profile evolution. For instance, models such as XBeach [11],

SBEACH [12] and LITPACK [13] were developed to study beach changes in a short-term period (hours, days) to investigate the impact of individual storms on the beach–dune system evolution and the response of beach fields under storm conditions. On the other hand, models such as Unibest-TC [14] were developed to study cross-shore evolution in the medium term [15]. In this work, cross-shore sediment transport processes are implemented by integrating the CS-Model [16] with the LTC model. The CS-Model is a simple model for characterizing the evolution of the cross-shore profile. It considers processes related to dune erosion, overwash, sediment transport by wind and exchange of sedimentary material between the bar and the berm [9,16]. The LTC model is based on the one-line theory and simulates medium- to long-term shoreline evolution considering natural and anthropogenic scenarios [4]. Other shoreline evolution models include GENESIS [17,18], Delft3D [19,20], Cascade [21,22], ONELINE [23] and the General Shoreline beach model [24,25]. The LTC model was developed by Coelho [4] and allows for the development of adaptations to include the combination of cross-shore and shoreline evolution capabilities. Integration of the two numerical models will help to better represent artificial nourishment behavior in the COAST tool.

Many calibration processes can be considered when applying cross-shore models. For example, XBeach can be calibrated with survey data before and after a storm event. XBeach parameter selection involves site-specific calibration to find the optimal values of each parameter [26]. A study by Simmons et al. [27] proposes another method to calibrate the SBEACH model, which can also be applied to other models. The GLUE method uses Monte Carlo sampling to evaluate the validity of combinations of model parameters to simulate an observed event and to further determine the model's skill for each run. This allows for the choice of an optimal parameter set for a simulation of an observed event. The LITPACK model was calibrated in the work of Paravath and Thuvanismail [28] using wave observations to calibrate wave transformation results. Simulations were performed including and excluding wind data, and the results match very well with the field data (including wind in simulations). Finally, the Unibest-TC model was used to simulate six years of observed wave data by Monecke et al. [29]. Their approach considered the first year to calibrate the model, using an initial profile. The profile after the one-year run was assumed to be in equilibrium, and simulations were performed with this calibrated model. Therefore, depending on the cross-shore model considered and the objectives of the study, there are a variety of model calibration approaches available. Factors that need to be considered when choosing the appropriate approach include limitations on the quantity, quality and extent of available datasets; relationships between the data used to calibrate and the data used to validate the models (in some cases, model validation is not considered) and the type and form of data considered in simulations (e.g., use of statistical analysis to choose best calibration parameters).

In this work, the CS-Model is selected to simulate an extensive dataset of forcing agents, and a calibration analysis is executed. In Marinho et al. [15], the CS-Model was used to simulate the evolution of multi-bar systems in the medium term. The model was calibrated for three different beaches in the United States (Duck, North Carolina; Silver Strand, California; Cocoa Beach, Florida) based on 4-, 2- and 1-year datasets, respectively. The results showed some potential to predict the evolution of two nearshore bars that migrate towards the shore and become part of the beach. Another example is presented in Hallin et al. [30], where the CS-Model was calibrated for 16 years of wave climate data and validated for 6 years for four beach profiles in Kennemer dunes (south of IJmuiden, the Netherlands). The impact of sediment supply on dune evolution was evaluated. Observations showed considerable variation in dune morphology, but the CS-Model was able to reproduce a large part of this variation.

The present study aims to discuss the CS-Model calibration process, supported by extensive datasets (about 40 years for IJmuiden and 10 years for Sand Motor) of forcing agents (wave climate, tides and wind) and beach profile data, analyzing model performance considering long-term simulations. The principal parameters of the CS-Model are compared

to the observed profiles, allowing for a discussion of the calibration process. Additionally, the impact of considering wave climate datasets derived from global and regional wave models for the IJmuiden study area is assessed, allowing for an evaluation of the importance of the wave regime on the final results. The next sections present the study areas (IJmuiden and Sand Motor), a description of the CS-Model and the available data considered, the results of the calibration process, a discussion of the importance of adequate wave climate definition and, finally, the main conclusions.

## 2. Study Area

The Netherlands has a 432 km long coastline, which comprises approximately 75% sandy beaches and dunes, 15% hard structures and 10% tidal flats [31]. The coastline can be subdivided into three different regions: the southwest delta, with multiple open and (semi-)enclosed estuaries; the central coast, relatively straight but with its orientation gradually changing from NE-SW in the south to N-S in the north (Holland coast); and the barrier island coast in the north, with multiple barrier islands and tidal inlets [32].

IJmuiden is located in the central part of the Holland coast and was selected as the study area (Figure 1) to take advantage of extensive monitoring works available from the area. The datasets encompass several parameters such as bathymetry/topography, waves, sediment grain size, shoreline position, coastal interventions, etc., covering long periods. Wave climate measurements were obtained from an offshore station (YM6 [33]: 52.55° N, 4.06° E) located 26 km from the IJmuiden coast, with a local depth of 21 m [34]. Typical wave height is registered between the values of 0.1 and 1.5 m (about 55.5% considering the period from January 1979 to December 2021). In the same period, wave direction comes predominately from the southwest (on average from 225 degrees counting north, clockwise). The tidal range at IJmuiden is about 1 m at neap tide and 2 m at spring tide [35]. Wave climate measurements at Sand Motor were obtained from the Euro-platform (EUR [33]: 52.00° N, 3.27° E), located at 30 m depth, at about 57 km from the coast [36]. Typical wave direction is mostly from the southwest and north-northwest, with an average significant wave height of 1 m in summer and 1.7 m in winter [37]. The tide is semi-diurnal, and tidal range varies between 1.4 m and 1.8 m over a spring-neap cycle [38].

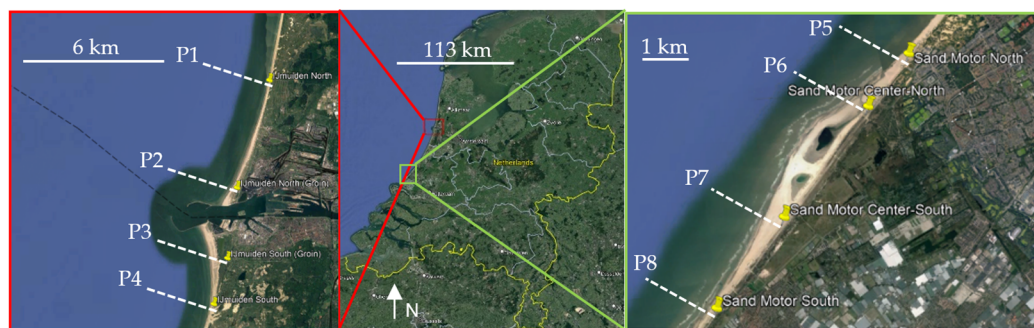


**Figure 1.** Location of the study areas along the central Holland coastline (**center**), with close-up view of profiles P1–P4 at IJmuiden (**left**) and profiles P5–P8 at Sand Motor (**right**).

Alongshore sediment transport is from south to north at both study areas. At IJmuiden, the beach to the south of the southern groin is an accretion area with an estimated 115,000–395,000 m<sup>3</sup>/year accretion rate. The beach north of the northern groin at IJmuiden has an observed erosion rate of about 40,000 m<sup>3</sup>/year [35]. However, the erosion is mitigated by regular artificial sand nourishments. At the Holland coast, annual average sand nourishment volumes have increased from 0.4 million m<sup>3</sup>/year in the period 1952–1990 to 2.5 million m<sup>3</sup>/year between 1991 and 2000 and have further increased to approximately 5 million m<sup>3</sup>/year from 2001 to the present [39]. Current annual mitigation costs are around EUR 25 million. Sand nourishments are commonly conducted in eroding coastal stretches, with added sand volumes around 200–600 m<sup>3</sup>/m [39].

To apply the CS-Model at the study areas, eight cross-shore profiles were chosen (see Figure 1): profiles P1 to P4 at IJmuiden and profiles P5 to P8 at Sand Motor. The profiles are named based on their position along the coast from north to south. Table 1 presents the conventional number attributed to the profiles and their coordinates.

**Table 1.** Name, conventional number and coordinates of the study area profiles.

Name	Conventional Number	Coordinates (Latitude; Longitude):
P1	7005450	52.513704° N; 4.592585° E
P2	7004975	52.472727° N; 4.572348° E
P3	8005750	52.445893° N; 4.566414° E
P4	8005950	52.428488° N; 4.557930° E
P5	9010527	52.067841° N; 4.216419° E
P6	9010338	52.059199° N; 4.204366° E
P7	9011018	52.041605° N; 4.180123° E
P8	9011221	52.027566° N; 4.161222° E

The location of profile P1 benefits from intermittent artificial nourishments around the coastal laboratory of Bergen–Egmond, and therefore, an accretion evolution is observed in the profile. These nourishments have been conducted since 1990, initially every two years, with deposited volumes between 60,000 and 1,472,640 m<sup>3</sup>. Between 1997 and 2000, the nourishments were conducted every year, and the deposited volumes were around 132,690–994,000 m<sup>3</sup>. In the period 2010–2015, artificial nourishments were spaced over 5 years, and the deposited sand volumes increased from 300,436 m<sup>3</sup> to 2,500,000 m<sup>3</sup> [40]. The south groin of IJmuiden works as a barrier to the longshore sediment transport that is predominant from south to north, promoting the accretion of sands in the southern area. Therefore, it is expected that both the P3 and P4 profiles benefit from the sediments trapped by the structure. The P2 profile is located in the shadow zone of the northern groin of the IJmuiden harbor entrance, so an erosion trend can be expected.

Sand Motor (south of Kijkduin, Figure 1) is the site of a large nourishment (mega-nourishment) performed from April to June 2011 on the southern part of the Holland coast. Approximately 21.5 million m<sup>3</sup> was deposited on the beach in a hook shape, forming a dune lake and an open lagoon on the landward side [41]. Sand Motor has received limited natural nourishments due to its location between two harbor entrances: the Scheveningen entrance to the north and the Hoek van Holland entrance to the south (Rotterdam harbor) [42]. The mega-nourishment dimensions are about 2.5 km alongshore and about 1 km in the cross-shore direction [41]. For the Sand Motor study area, it was anticipated that a large section of the neighboring coastline would benefit from the deposited sediments at the mega-nourishment site, as they would be distributed by diffusion processes over time. This intervention causes a barrier effect on the alongshore sediment transport, and therefore, profiles P7 and P8, located downdrift of the nourishment, would also benefit from sediments coming from the south that get trapped by the barrier. Profiles P5 and P6 would benefit from the natural diffusion of sediments due to the alongshore sediment transport.

The sediment grain size (median diameter, d50) at IJmuiden is between 0.20 and 0.25 mm. At Sand Motor, the typical sediment grain size is the same as encountered in the IJmuiden area, and alongshore sediment transport is about 180,000 m<sup>3</sup>/year (from south to north) in the area [35].

### 3. Materials and Methods

The CS-Model was used to simulate the cross-shore evolution of the beach profiles after calibration with real data from IJmuiden and Sand Motor. The measured datasets include profile evolution between 1965 and 2022 and 2011 and 2022, wave climate between 1971 and 2022 and 2011 and 2021 and tide levels between 2002 and 2022 and 2000 and 2019 for IJmuiden and Sand Motor, respectively. Considering the combined range of the available data, the time periods of analysis were defined between 1979 and 2020 for the

IJmuiden study area and 2011 and 2021 for Sand Motor (tide levels were replicated and extended to past periods to complete the time range in accordance with the other data).

In this section, the CS-Model and the available data for each study area are described. All morphological parameters considered in the CS-Model are described in Section 3.1. Available profile data and forcing agents data are defined in Sections 3.2 and 3.3, respectively. In Section 3.4, the initial model parametrization is presented, based on the data approximation to the model conditions. After defining the initial conditions for simulations, namely the simplified geometrical parametrization of each profile, different modeling parameters were tested for calibration. Finally, in Section 3.5, the wave climate data derived from global wave models are presented. These data were tested under the calibration assumptions of the observed wave climate.

### 3.1. CS-Model

Figure 2 represents the simplified scheme of a typical profile in the CS-Model: the position of the dune toe, both land- and seaward ( $Y_L$  and  $Y_S$ , respectively); the position of the berm ( $Y_B$ ); the position of the shoreline ( $Y_G$ ); the dune height ( $S$ ); the berm height ( $D_B$ ); the closure depth ( $D_C$ ); the slope of the dune ( $\beta_L$  and  $\beta_S$ , land- and seaward, respectively) and the beach slope ( $\beta_B$ ). The model considers sediment exchanges between the dune and the berm due to runup and overtopping ( $q_S$ ) and between the berm and the bar ( $q_B$ ) so that an initial value of bar volume ( $V_B$ ) can also be given. The aeolian sediment transport allows definition of dune volume growth or loss to the beach ( $q_{WS}$  and  $q_{WL}$ , in seaward and landward direction, respectively) [16].

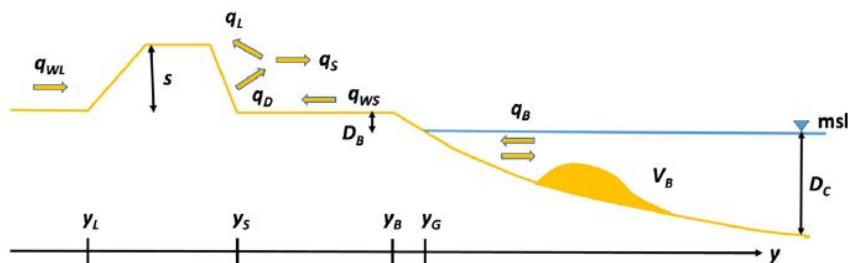


**Figure 2.** Schematized cross-shore profile in CS-Model: parameters used to create the shape of the profile ( $Y_L$ ,  $Y_S$ ,  $Y_B$ ,  $Y_G$ ,  $S$ ,  $D_B$  and  $D_C$ ), bar volume ( $V_B$ ), berm–bar exchanges ( $q_B$ ), sediment removed from the dune ( $q_D$ ) divided into a seaward and landward component ( $q_S$  and  $q_L$ ) and wind-blown sand that will contribute to dune growth ( $q_{WL}$  in landward direction and  $q_{WS}$  in seaward direction) [16].

The governing equations of the bar, berm and dune evolution in the sea- and landward directions were previously defined by Larson et al. [16], following Equations (1)–(4).

$$\frac{\partial V_B}{\partial t} = q_B \quad (1)$$

Equation (1) controls interaction between the berm and bar such that if sand is eroded from the berm, the bar grows, and if sand is eroded from the bar, the berm position advances in the offshore direction [16].

$$\frac{\partial Y_B}{\partial t} = \frac{1}{D_B + D_C} \left( -q_{ws} - q_B + q_S - \frac{\partial Q_L}{\partial x} \right) \quad (2)$$

Equation (2) controls bar–berm material exchange (Equation (1)), aeolian sediment transport towards the dune ( $q_{WS}$ ), seaward transport resulting from erosion of the dune ( $q_S$ ) and the gradient of longshore sediment transport ( $\frac{\partial Q_L}{\partial x}$ ) causing advancement or retreat of the shoreline [16].

$$\frac{\partial Y_S}{\partial t} = \frac{-q_D + q_{ws}}{S} \quad (3)$$

$$\frac{\partial Y_L}{\partial t} = \frac{-q_L - q_{wL}}{S} \quad (4)$$

Dune evolution depends on wave impact and dune build-up from wind (seaward side) and build-up from overwash and aeolian transport (landward side) [16]. For calibration purposes, the dune foot seaward ( $Y_S$ ) and berm ( $Y_B$ ) positions were chosen to be the principal morphological parameters to be evaluated.

### 3.2. Profile Data

From all profiles available at IJmuiden and Sand Motor, four were chosen to represent each site (Figure 1). At IJmuiden, two of the profiles are located south of the harbor entrance and two north of the entrance. All four profiles had available annual data from 1965 to 2022 (P1 to P4, Figure 3). For Sand Motor, two profiles are located north (updrift) of the center of the mega-nourishment and two profiles south of it (downdrift). The monitoring period considered for the profiles was 2011 to 2022 (P5 to P8, Figure 4).

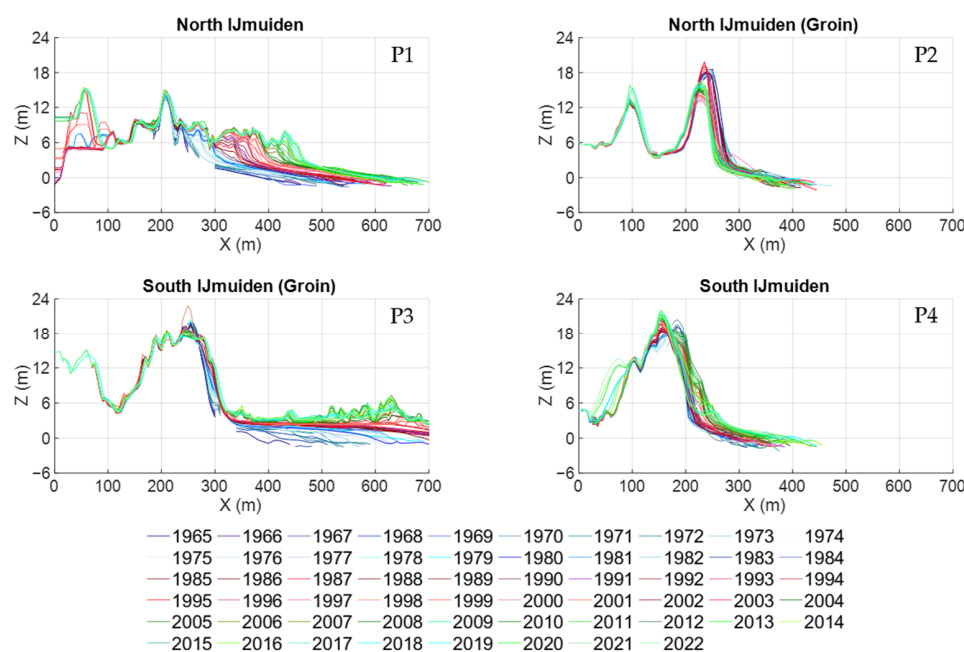


**Figure 3.** Beach profile data at IJmuiden study area (1965–2022).

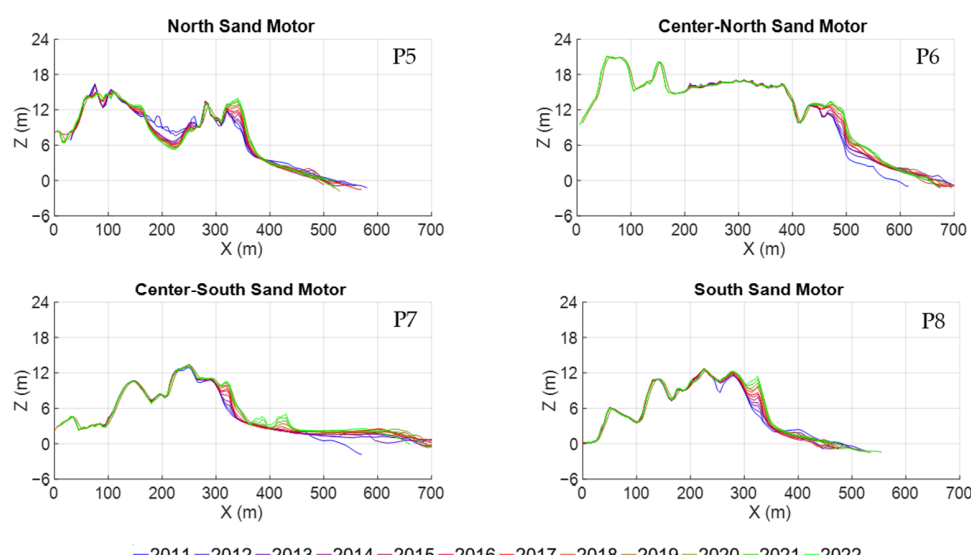


**Figure 4.** Beach profile data at Sand Motor study area (2011–2022).

### 3.3. Forcing Agents Data

All the forcing agents are represented in Figure 5, including the wave climate (YM6 dataset) between 1979 and 2022 (the available time series ranges from 1971 to 2022). The data considered included the wave height ( $H$ ) in meters, wave period ( $T$ ) in seconds, wave direction ( $\text{Dir}$ ) in degrees (counting north, clockwise) and tide levels (tide) in meters (tide range was replicated and extended to past periods to complete the same period). The Sand Motor wave climate data (EUR dataset) also contain a time range between 1971 and 2021, but only the period between 2011 and 2021 was selected, representing the data available after the construction of the mega nourishment.

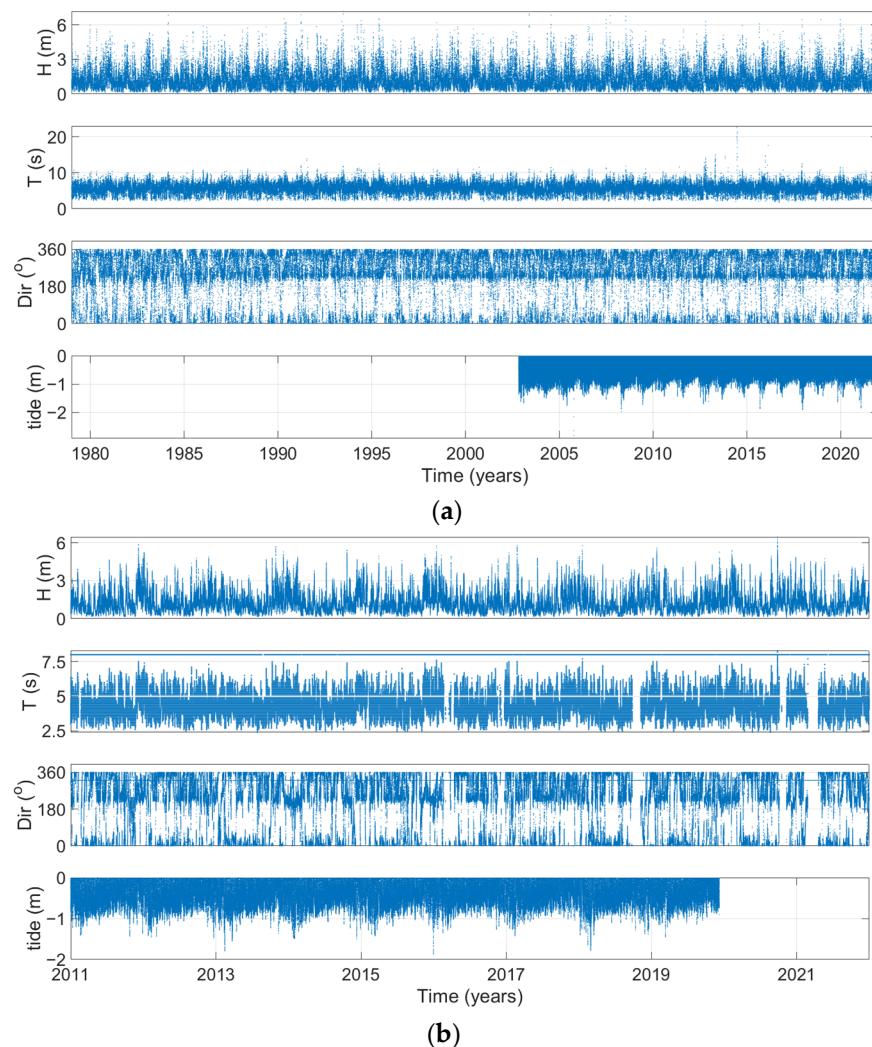


**Figure 5.** Forcing agents data series (offshore wave parameters and tide levels): (a) IJmuiden study area; (b) Sand Motor study area.

### 3.4. Initial Modeling Conditions

At IJmuiden, the first available cross-shore profile (1979) was used to define the initial profile scheme to be considered in the CS-Model simulations. Based on the surveyed period and forcing agents, the simulation time horizon adopted in the calibration process represents the period between 1979 and 2020. The wave climate and tide levels were interpolated to have all data in coincident time periods. Therefore, the CS-Model simulations considered a period of 41 years (1979–2020) forced by 3-h wave climate time series (time step of the simulations). At the Sand Motor study area, the same process was considered, but the initial profile represents 2011 (year when the mega-nourishment was constructed) and the wave climate data cover a period of 10 years (2011–2021). In the same way as

IJmuiden, data were interpolated to be coincident at a 3-h time step, and tide range data were replicated to the most recent years to complete the time series.

The initial cross-shore profiles (1979 for IJmuiden and 2011 for Sand Motor) and their CS-Model scheme approximations are represented in Figure 6, allowing definition of the initial landward and seaward dune toe positions ( $Y_L$  and  $Y_S$ , respectively) and the initial position of the berm ( $Y_B$ ). At P2, two profiles were approximated by the CS-Model with variation in the initial shape, mainly related to the berm height ( $D_B$ ).

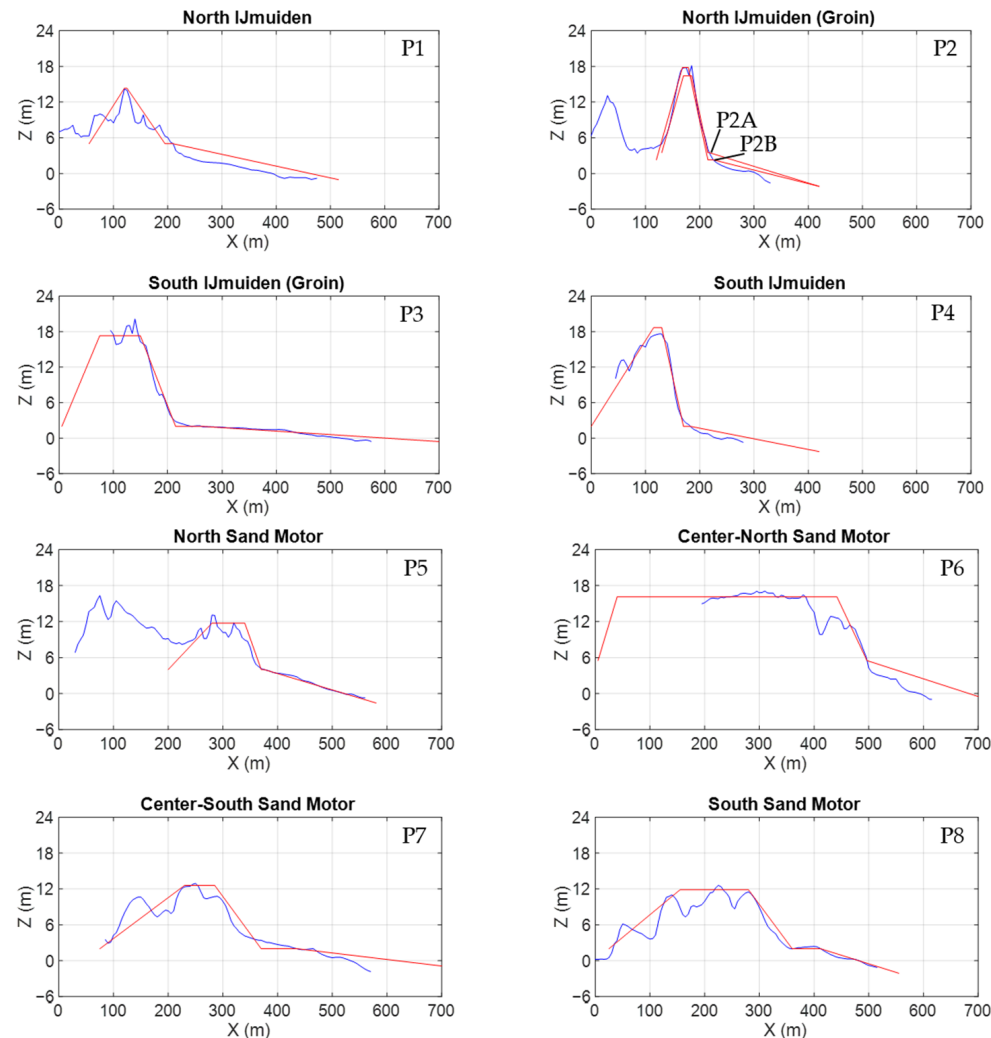


**Figure 6.** Study areas' initial profile (blue) and CS-Model scheme approximation (red).

Table 2 presents an overview of the initial parametrization of the CS-Model, considering the years 1979 for IJmuiden and 2011 for Sand Motor. The dune face slopes ( $\beta_L$  and  $\beta_R$ , land- and seaward, respectively) and the berm slope ( $\beta_B$ ) were calculated considering the mean slope of all the profiles of each location (P1 to P8). Table 3 presents the slopes considered for each profile. From the available profiles it is possible to observe the evolution of profile parameters between 1979 and 2020 in IJmuiden and between 2011 and 2021 in Sand Motor, providing a challenging calibration process for the CS-Model of the berm and dune position with time and the exchanged sediment volumes between the bar and the berm and between the berm and the dune. The calibration process considered coefficients to represent wind-blown sand transport, wave run-up friction, dune attack and overwash and berm–bar sediments exchange.

**Table 2.** Land- and seaward dune foot positions ( $Y_L$  and  $Y_S$ , respectively), berm position ( $Y_B$ ), dune height (S) and berm height ( $D_B$ ), all in meters, for each initial profile considered in CS-Model.

Profile	P1	P2A	P2B	P3	P4	P5	P6	P7	P8
$Y_L$	55.00	130.00	120.00	5.00	0.00	200.00	5.00	75.00	25.00
$Y_S$	195.00	215.00	215.00	215.00	170.00	370.00	496.74	370.00	360.00
$Y_B$	210.00	217.82	224.75	263.13	182.70	375.45	496.74	435.42	411.90
S	9.32	12.92	15.50	15.30	16.67	7.74	10.63	10.60	9.87
$D_B$	5.00	3.50	2.30	2.00	2.00	4.00	5.50	2.00	2.00

**Table 3.** Dune face slopes land- and seaward ( $\beta_L$  and  $\beta_S$ , respectively) and berm slope ( $\beta_B$ ) for each profile, all in radians, considered in CS-Model.

Profile	P1	P2A	P2B	P3	P4	P5	P6	P7	P8
$\beta_L$	0.4361	0.3124	0.3124	0.2152	0.1465	0.0964	0.2949	0.0683	0.0758
$\beta_S$	0.1324	0.4067	0.4067	0.2312	0.3949	0.2525	0.1909	0.1241	0.1228
$\beta_B$	0.0246	0.0279	0.0228	0.0108	0.0195	0.0278	0.0336	0.0115	0.0222

The best calibration results, especially in the seaward dune foot position ( $Y_S$ ) and berm position ( $Y_B$ ) for the IJmuiden and Sand Motor study area, were evaluated by statistical analysis of the differences between observed and modeled profile characteristics with time, through the Mean Absolute Error (MAE) defined by Equation (5).

$$MAE = \frac{1}{N} \sum_{i=1}^n |P_i - O_i| \quad (5)$$

Mean absolute error represents the mean of the absolute error that shows the differences between the values simulated with the CS-Model ( $P_i$ ) and the observed values ( $O_i$ ). The best model performance of  $Y_B$  and  $Y_S$  was obtained by changing input parameters related to aeolian sediment transport (QWINDS), dune erosion volumes after wave impacts (CIMPACT) and accretion rate (AR) while maintaining other parameters. After calculating the mean absolute error of  $Y_B$  and  $Y_S$  from the IJmuiden study area considering the YM6 dataset, the results were compared with other datasets. The mean absolute errors for 10-year periods were also estimated, allowing for evaluation of fluctuations in the model's performance with time. Finally, considering the MAE, the Mean Relative Error (MRE) to the total movement of the evaluated positions of the berm and the seaward dune toe was quantified (Equation (6)).

$$MRE = \frac{MAE}{|O_n - O_1|} \quad (6)$$

After defining the calibrated conditions to simulate the evolution of the profiles, both for IJmuiden (P1 to P4) and Sand Motor (P5 to P8), the modeling performance at IJmuiden was compared with the results in the Sand Motor region where a shorter calibration period of data was considered. The impact of the different wave climate data available at IJmuiden was also evaluated. Remarks on these results are highlighted below.

### 3.5. Wave Climate Data from Global and Regional Models

Wave climate datasets derived from global and regional wave models were collected for the IJmuiden area and used to evaluate the influence of different sources of data in the calibrated model. The global model datasets used were the reanalyzed data from the global ERA5 model [43] and hindcast simulations from the regional AENWS-WPR model [44]. The ERA5 database represents a point close to the initial measured point YM6 (ERA5: 52.5° N, 4.0° E). The AENWS-WPR model was used to generate wave climate data at the

location  $52.55^{\circ}$  N,  $4.06^{\circ}$  E (location of YM6) and for two points close to shore, one north of IJmuiden ( $52.51^{\circ}$  N,  $4.55^{\circ}$  E) and the other south of IJmuiden ( $52.42^{\circ}$  N,  $4.52^{\circ}$  E) [45]. The position of the datasets considered is shown in Figure 7. Wave roses for each dataset are presented in Figure 8.

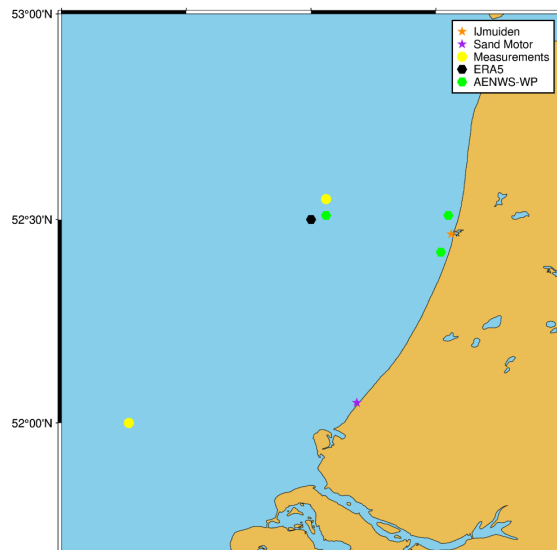


**Figure 7.** Location of wave datasets derived from global models compared with the measured datasets (YM6, EUR) near IJmuiden and Sand Motor [45].

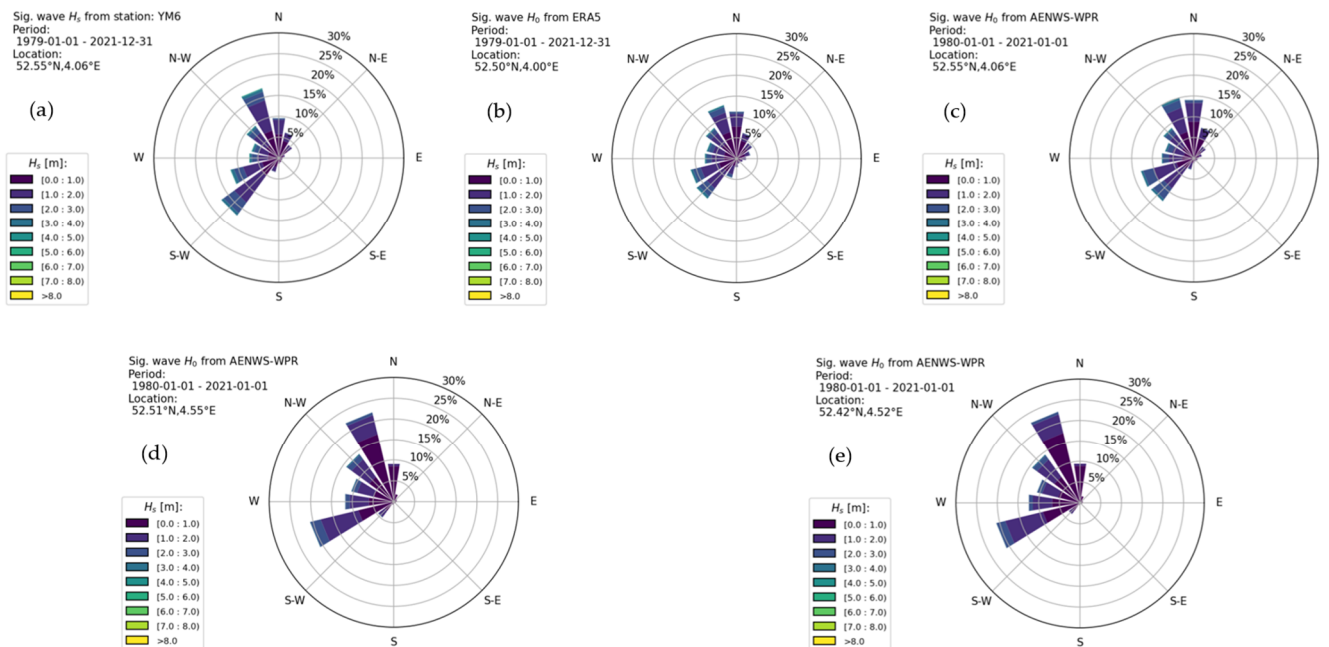


**Figure 8.** Wave roses for different datasets at IJmuiden: (a) YM6, (b) ERA5, (c) AENWS-WPR, (d) AENWS-WPR at the northern shoreline point and (e) AENWS-WPR at the southern shoreline point.

A statistical analysis of the wave climates is presented in Table 4, showing the main differences in the datasets. The mean direction is mainly from the southwest quadrant (180–270 degrees). The maximum offshore wave height ranges from 6.46 m at Sand Motor (EUR) to 7.47 m at the ERA5 dataset point at IJmuiden. The maximum wave height at the shoreline is 4.23 m and 4.56 m at the southern and northern points at IJmuiden, respectively. The maximum wave periods are much higher at IJmuiden than at Sand Motor.

**Table 4.** Statistical analysis of wave height, wave period and wave direction for analyzed datasets at IJmuiden (YM6, ERA5, AENWS-WPR) and Sand Motor (EUR).

Variable	Database	Mean	std	Max	Min
H (m)	YM6	1.27	0.83	7.17	0.09
	ERA5	1.20	0.79	7.47	0.03
	AENWS-WPR	1.24	0.76	6.72	0.03
	AENWS-WPR Shore: North	0.94	0.64	4.56	0.02
	AENWS-WPR Shore: South	0.90	0.61	4.23	0.02
	EUR	1.23	0.76	6.46	0.11
T (s)	YM6	5.68	1.35	22.97	1.79
	ERA5	5.97	1.85	19.35	1.83
	AENWS-WPR	6.33	1.98	18.85	1.65
	AENWS-WPR Shore: North	6.42	2.14	19.52	1.65
	AENWS-WPR Shore: South	6.40	2.12	19.57	1.65
	EUR	4.68	1.34	8.30	2.40
Dir (°)	YM6	235.39	104.57	-	-
	ERA5	223.22	110.14	-	-
	AENWS-WPR	230.66	112.83	-	-
	AENWS-WPR Shore: North	276.00	77.96	-	-
	AENWS-WPR Shore: South	279.09	75.92	-	-
	EUR	218.75	115.64	-	-

Additionally, the wave height for each wave quadrant (only the relevant quadrants are presented) was also evaluated by considering different percentiles of occurrence (Table 5). In accordance with Figure 8, SW and NW quadrants registered the most incoming waves. It is highlighted that nearshore wave databases (AENWS-WPR Shore: North and AENWS-WPR Shore: South) present much lower wave heights. Comparing YM6, ERA5 and AENWS-WPR for offshore sites at IJmuiden, the analysis shows a higher absolute difference for the higher percentiles. Comparison of the measured wave height at YM6 and the modeled wave height from the ERA5 and AENWS-WPR datasets indicates that there is not a clear trend showing that the modeled wave data over- or underestimate wave height when compared to the observed values.

**Table 5.** Wave height (m) per wave direction for all databases considering different percentiles of occurrence.

Direction	%	YM6	ERA5	AENWS-WPR	AENWS-WPR Shore: North	AENWS-WPR Shore: South	EUR
N (20899)	25	0.54	0.49	0.50	0.33	0.32	0.55
	50	0.79	0.74	0.78	0.45	0.45	0.82
	75	1.13	1.07	1.13	0.60	0.59	1.14
	90	1.52	1.49	1.53	0.79	0.79	1.56
	99	2.46	2.64	2.58	1.17	1.15	2.74
NW (50642)	25	0.75	0.67	0.73	0.54	0.52	0.70
	50	1.24	1.07	1.21	0.90	0.87	1.06
	75	1.89	1.66	1.85	1.37	1.33	1.71
	90	2.70	2.44	2.60	1.94	1.88	2.43
	99	4.57	4.21	4.08	3.19	3.07	3.97
W (37363)	25	0.73	0.74	0.79	0.62	0.60	0.65
	50	1.29	1.20	1.28	1.00	0.97	1.10
	75	2.03	1.88	1.91	1.49	1.43	1.78
	90	2.87	2.66	2.54	2.03	1.94	2.53
	99	4.54	4.25	3.64	2.99	2.84	3.94

**Table 5.** Cont.

Direction	%	YM6	ERA5	AENWS-WPR	AENWS-WPR Shore: North	AENWS-WPR Shore: South	EUR
SW (56651)	25	0.85	0.82	0.95	0.67	0.62	0.88
	50	1.30	1.31	1.44	1.10	1.04	1.35
	75	1.91	1.96	2.04	1.58	1.52	1.95
	90	2.56	2.64	2.60	2.03	1.96	2.61
	99	3.74	3.92	3.51	2.78	2.67	3.73

#### 4. Results

This section is subdivided into three parts: firstly, the calibration process for the IJmuiden study area is considered using the YM6 dataset; secondly, different wave climate datasets are applied to the simulation at IJmuiden to evaluate effects on final results; and thirdly, the calibration of the Sand Motor study area is presented using the EUR dataset. The results of both areas are then compared, allowing for discussion of the performance of about 40 years and 10 years of data to support the calibration. Some remarks are presented in a final subsection.

##### 4.1. Calibration Process of IJmuiden Using YM6 Dataset

The parameters used to compare the differences between the observed and the modeled values were dune height ( $S$ ), seaward dune toe position ( $Y_S$ ), berm position ( $Y_B$ ) and bar volume ( $V_B$ ). In profiles P1, P3 and P4, the dune characteristics were maintained along the time horizon of analysis, and thus,  $S$  and  $Y_S$  should be fixed, and  $Y_B$  was observed to advance in the offshore direction. A constant accretion rate that best represented the evolution of the berm position ( $Y_B$ ) was used. Important changes in  $V_B$  are difficult to represent in the model in a long-term analysis and thus were not considered as a calibration parameter. Therefore, an initial value of  $V_B$  was taken to be equal to the initial observed value. Due to difficulties in representing the best behavior, two different representative characteristics were defined in the P2 location (simulations of profiles P2A and P2B), changing the berm height ( $D_B$ ) and the berm slope ( $\beta_B$ ). In this profile, the calibration goal was to represent the decrease in the dune height ( $S$ ) and the retreat of the seaward dune toe ( $Y_S$ ) and the berm ( $Y_B$ ) positions. After a first try considering a constant accretion rate at P3 (P3A), the calibration of profile P3 adopted a division of the profile behavior in two parts with time (P3B) to have a better approximation of the modeled  $Y_B$ , as the observed  $Y_B$  tended to present an important accretion rate up until 1997, decreasing in intensity after that. This behavior may result from an intense accumulation of sand due to the breakwater works during the first period and a later less intense accumulation when the deposition area was almost filled by sand. Therefore, the first part has an accretion rate (AR) of  $8.4 \times 10^{-6}$  m/time step (2.45 cm/year), and the second part an AR =  $1.1 \times 10^{-6}$  m/time step (0.32 cm/year). This profile was modeled between 1979 and 1997 with the first-year profile, and the results of morphological parameters were used as inputs for the second time range (1997–2020). The complicated offshore conditions (between 500 and 700 m depth) were approximated by defining a medium slope considering the time range of the analysis. The oscillations were considered to be part of the submerged bar volumes. For profiles P1 and P4, the calibration process was simpler, requiring only a single value of AR for both profiles, resulting in only one calibration approach for each profile. Table 6 summarizes the values adopted for each parameter for the IJmuiden study area. The principal parameters in the CS-Model that affect morphological changes are QWINDS, which represents the flow rate of aeolian sediment transport (in  $m^3/s/m$ ), and CIMPACT, a coefficient that is used to calculate the volume of sediment removed from the dune when the wave directly hits it. In this work, aeolian transport was estimated in the calibration process and considered constant throughout all simulations.

**Table 6.** Adopted QWINDS ( $\text{m}^3/\text{s}/\text{m}$ ), CIMPACT and accretion rate (AR,  $\text{m}/\text{time step}$ ) in the CS-Model for each profile (P1 to P4).

Profile	P1	P2A	P2B	P3A	P3B	P4
QWINDS	$9.3 \times 10^{-8}$	$5.0 \times 10^{-11}$	$1.0 \times 10^{-9}$	$9.1 \times 10^{-8}$	$9.2 \times 10^{-8}$	$2.7 \times 10^{-7}$
CIMPACT	$1.0 \times 10^{-4}$	$1.0 \times 10^{-4}$	$1.0 \times 10^{-5}$	$1.0 \times 10^{-6}$	$1.0 \times 10^{-6}$	$1.0 \times 10^{-5}$
AR	$2.4 \times 10^{-6}$	$-7.0 \times 10^{-7}$	$-6.0 \times 10^{-7}$	$5.7 \times 10^{-6}$	*	$7.0 \times 10^{-7}$

\* AR =  $8.4 \times 10^{-6}$  m/time step up until 1997 and AR =  $1.1 \times 10^{-6}$  m/time step afterwards.

Table 7 shows the mean absolute error obtained after calibration (according to Equation (1)) for  $Y_B$  and  $Y_S$  using the YM6 dataset, compared with observations. The results of  $Y_B$  and  $Y_S$  evolution are presented in Figures 9 and 10, respectively, and also include the analysis of the behavior when another wave climate is adopted.

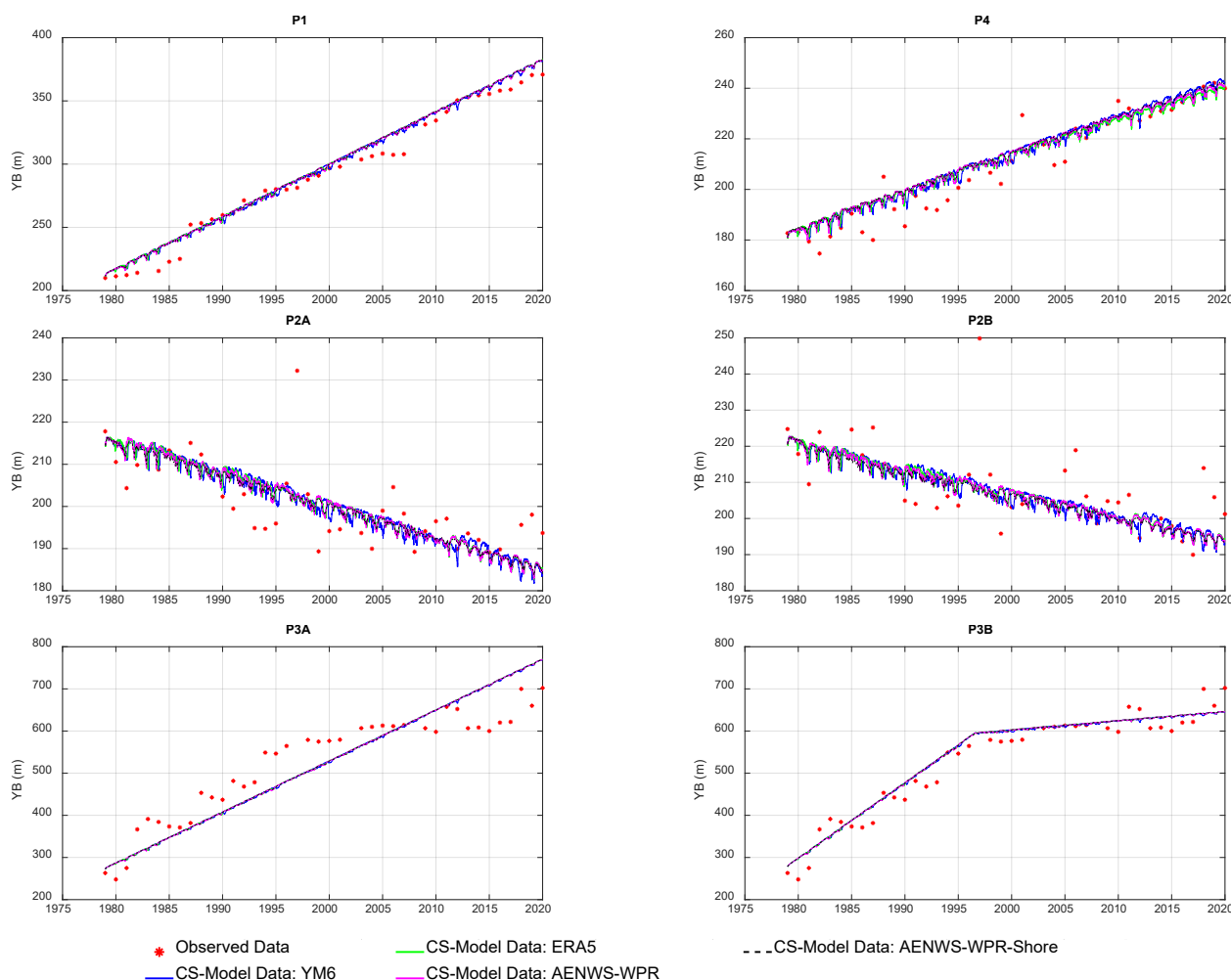


**Figure 9.** Evolution of modeled and observed values of berm position ( $Y_B$ ).

Table 7 shows that the simulated trends of evolution of the berm position compare well with observations, with the mean absolute errors being lower than 6.30 m in all profiles except P3. Profile P3A shows a mean absolute error of 49.75 m, and after dividing it into two parts, the results show better approximations of  $Y_B$  (mean absolute error of 23.30 m) despite it being the worst profile approximation. The intense accretion at P3 (the profile position benefiting from the deposition of sediments being trapped by the breakwater) is difficult to reproduce in the CS-Model. For the seaward dune foot position, the results are better as all profiles have mean absolute errors less than or equal to 4.25 m.

Considering both approaches developed for profile P2, the P2A scheme better represents the performance of the berm position. However, the P2B scheme shows a better representation of the seaward dune toe position.

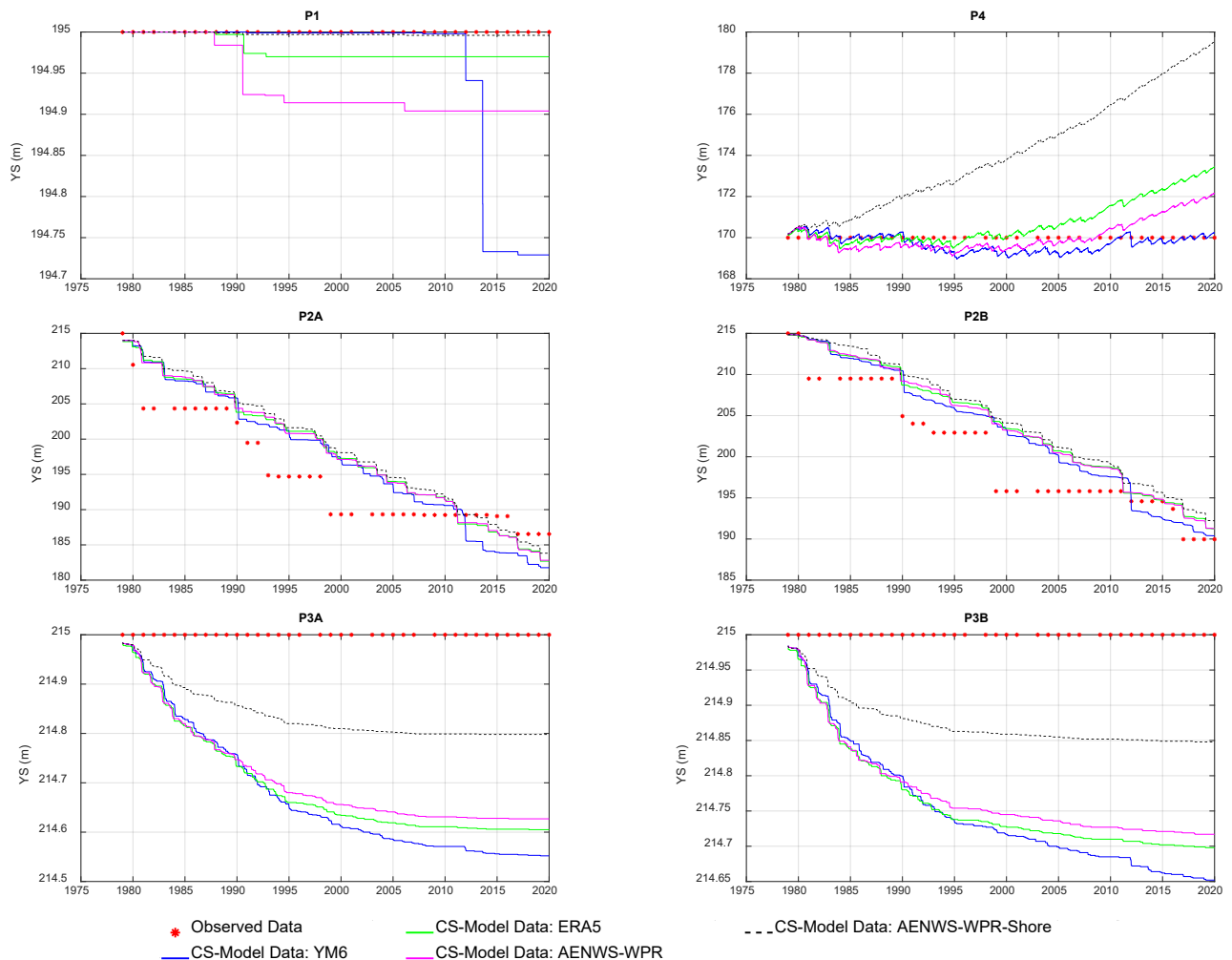


**Figure 10.** Evolution of modeled and observed values of seaward dune foot position ( $Y_S$ ).

**Table 7.** Mean absolute error of  $Y_B$  and  $Y_S$  for each profile using YM6 dataset and compared with observed values at the IJmuiden study area.

Mean Absolute Error (m)	P1	P2A	P2B	P3A	P3B	P4
$Y_B$	5.39	5.54	6.30	49.75	23.30	5.47
$Y_S$	0.05	4.25	3.03	0.32	0.24	0.38

#### 4.2. Wave Climate Effects at IJmuiden

In Figure 9, the evolution of the berm position ( $Y_B$ ) is represented for each profile considering the adequate accretion rate, QWINDS and CIMPACT for the YM6 wave climate and repeating these same calibration values for the other wave climate series.

All wave climate datasets for each IJmuiden profile resulted in similar behaviors. For P1 and P3 (both P3A and P3B approaches), the predominance of the long-term behavior does not allow for adequate representation of the eventual impact of specific events on the berm position ( $Y_B$ ) for all datasets considered. According to Guillén et al. [46], accretion trends in the dune foot position are observed between 1965 and 1992, showing an advancement in shoreline position. In P2A, the simulated values of  $Y_B$  for all datasets

reproduced relatively well the observed position retreat, e.g., during the years 1984, 1990 and 2008. Considering P2B, the retreat of  $Y_B$  was simulated for 1984, 1995, 2012 and 2013 in accordance with observed data. Finally, for profile P4,  $Y_B$  retreat was simulated for 1981, 1983, 1984, 1991, 1995, 2012, 2013, 2014 and 2015 which corresponds to the observed data. In Table 8, the mean absolute error representing the average difference between the results and the observed profile characteristics was calculated for each dataset. The results show the same behavior for different datasets at the same profiles.

**Table 8.** Mean absolute error (MAE) and mean relative error (MRE) of  $Y_B$  for each dataset and for each IJmuiden profile.

Profile	YM6		ERA5		AW *		AWN *		AWS *	
	MAE (m)	MRE (%)								
P1	5.39	3.35	5.79	3.60	5.87	3.65	5.84	3.63	-	-
P2A	5.54	22.97	5.43	22.51	5.38	22.31	5.27	21.85	-	-
P2B	6.30	26.77	6.13	26.05	6.04	25.67	6.15	26.14	-	-
P3A	49.75	11.33	50.41	11.48	50.70	11.55	-	-	50.56	11.52
P3B	23.30	5.31	23.10	5.26	23.39	5.33	-	-	23.38	5.33
P4	5.47	9.55	5.00	8.73	4.82	8.41	-	-	5.06	8.83

\* AW = AENWS-WPR dataset; AWN = AENWS-WPR-Shore (North); AWS = AENWS-WPR-Shore (South).

Profile P1 showed a mean absolute error of 5.39 m in the calibrated scenario which used the YM6 dataset. For P2A, the best scenario had a mean absolute error of 5.27 m and was achieved with the AENWS-WPR-Shore (North) dataset. When berm height decreased from 3.5 m to 2.3 m (P2B), the best scenario was achieved using the AENWS-WPR dataset (mean absolute error equal to 6.04 m). The P3 profile presented two trends over the total simulated period. The P3A profile had the worst mean absolute error, with the best performance of 49.75 m being achieved using the YM6 dataset. P3B was simulated in two parts using different input parameters corresponding to the change in the trend. The results were the best (MAE = 23.10 m) with the ERA5 dataset. It is important to notice that the relative errors obtained for this profile are of the same magnitude as the other profiles, with the P3B option having the second lowest mean relative error. Finally, for the P4 profile, the best scenario was achieved using the AENWS-WPR dataset, with a mean absolute error of 4.82 m. The MRE of each profile is almost independent of the dataset considered, as the mean errors were similar. In conclusion, when comparing the  $Y_B$  evolution simulated from different wave climate datasets, the differences in the mean errors are minimal. This allows for the conclusion that using available global datasets such as ERA5 does not significantly change the final profile shape compared to using measured data.

Figure 10 represents the evolution of the  $Y_S$  parameter. For profile P1, YM6 data showed a major variation in dune foot position on the seaward side ( $Y_S$ ), but the maximum difference was only 0.27 m in 2020 when compared with observations. In this profile, the best results were achieved when applying the AENWS-WPR-Shore dataset (differences about 1 mm).

Profile P2 presented the worst performance when simulating  $Y_S$ . For P2A using the YM6 dataset, the final results showed a difference of 4.78 m for observation values, and better results were observed when considering the AENWS-WPR-Shore dataset, with a difference of 2.72 m. For P2B, the best results were achieved using the YM6 dataset (differences to observed data of 0.40 m), and the worst scenario was with the AENWS-WPR-Shore dataset with a difference of 2.24 m.

Considering both approaches for profile P3 (P3A and P3B), the best results were achieved using the AENWS-WPR-Shore dataset, with differences of 0.20 m and 0.15 m in 2020, respectively, compared with observations. The worst scenarios used the YM6 dataset, with values of 0.45 m and 0.35 m, respectively. Finally, for profile P4 in 2020, the best results were achieved using the YM6 dataset, with differences of 0.25 m. Using the AENWS-

WPR-Shore dataset, the differences increased to 9.54 m compared with observations. The big changes in this profile can be explained considering that the wave climate initially does not hit the dune foot. The calibration of  $Y_B$  and  $Y_S$  was specially challenging for this profile as  $Y_S$  should keep its position with time, and therefore, the QWINDS value needs to compensate for the dune erosion caused by wave attack at the dune. As AENWS-WPR-Shore presents reduced wave heights (see Table 5), the effects of aeolian sediment transport are not compensated for by dune erosion, and an accretion behavior is observed from 1980 onward. With the ERA5 wave dataset, higher waves allow some dune erosion, and the seaward dune toe movement is observed later (around 2000). Finally, the AENWS-WPR dataset starts to increase the  $Y_S$  position in 2008 due to higher waves and dune erosion.

The simulations aimed to maintain the value of  $Y_S$  when accretion was observed in the profile and represent the dune retreat in the case of profile erosion and dune wave attack. Keeping  $Y_S$  fixed can be easily achieved by reducing the CIMPACT parameter to zero (decreases the impact of waves in the dune) and reducing the wind parameter to zero (not allowing aeolian sediment transport). However, in these conditions, the CS-Model would represent a profile with a fixed position of the dune. In conclusion, the best results were mainly achieved when applying AENWS-WPR-Shore dataset (four cases), which performed better than the model calibrated with the YM6 dataset. The mean absolute and relative errors of the simulated dune foot seaward position are presented in Table 9 for all IJmuiden profiles. As no variation in the dune foot position was observed in profiles P1, P3 and P4, their mean relative error is not presented.

**Table 9.** Mean absolute error (MAE) and mean relative error (MRE) of  $Y_S$  for each dataset and for each IJmuiden study area profile.

Profile	YM6		ERA5		AW *		AWN *		AWS *	
	MAE (m)	MRE (%)								
P1	0.05	-	0.02	-	0.07	-	0.00	-	-	-
P2A	4.25	14.93	4.29	15.07	4.19	14.72	4.50	15.81	-	-
P2B	3.03	12.11	3.65	14.58	3.52	14.06	4.23	16.90	-	-
P3A	0.32	-	0.30	-	0.29	-	-	-	0.16	-
P3B	0.24	-	0.23	-	0.22	-	-	-	0.12	-
P4	0.38	-	0.82	-	0.59	-	-	-	3.98	-

\* AW = AENWS-WPR dataset; AWN = AENWS-WPR-Shore (North); AWS = AENWS-WPR-Shore (South).

All datasets show similar results, with the mean absolute error varying by a maximum of 1.20 m in P2B simulations (3.03 m for YM6 compared to 4.23 m for AENWS-WPR-Shore). In P1, the best result was obtained using the AENWS-WPR-Shore dataset, with a mean absolute error very close to 0.00 m. The P2A profile presented a mean absolute error of 4.19 m (best result) when the AENWS-WPR dataset was used. For the P2B profile, the best result was achieved using the YM6 dataset, with a mean absolute error of 3.03 m. The mean relative error of this simulation is of the same magnitude as the errors observed for the berm position which are similar for all wave datasets. In the P3A profile, the mean absolute error was about 0.16 m using the AENWS-WPR-Shore dataset (best scenario), and this same dataset achieved the best result in P3B, with a mean absolute error of 0.12 m. Finally, for profile P4, the best result was achieved with the YM6 dataset, with a mean absolute error of 0.38 m. Therefore, YM6 and AENWS-WPR-Shore are the datasets with the best performances, while ERA5 never presented the lowest mean absolute error of the results.

#### 4.3. Calibration Process of Sand Motor Using EUR Dataset

Table 10 presents the values of QWINDS ( $m^3/s/m$ ), CIMPACT and accretion rate (AR, m/time step) adopted to calibrate each profile of Sand Motor (P5 to P8). Trying to achieve a lower mean absolute error in profile P7, the simulations firstly considered all the years and an accretion rate of  $1.10 \times 10^{-5}$  m/time step (P7A). Later, the first two years of simulation

were ignored due to their different behavior, and simulations were then started in 2013 (P7B) with an accretion rate of  $4.40 \times 10^{-6}$  m/time step. Profile P8 was also difficult to calibrate; therefore, after a first try considering all the calibration parameters constant along the simulation (P8A), the simulations were divided in two periods considering different values of QWINDS, CIMPACT and AR (P8B, part I from 2011 to 2016 and part II from 2016 to 2021). Profiles P5 and P6 considered one value of AR in the calibration process to represent best evolution of  $Y_B$  and  $Y_S$ .

**Table 10.** Adopted QWINDS ( $\text{m}^3/\text{s}/\text{m}$ ), CIMPACT and accretion rate (AR, m/time step) in the CS-Model for each profile (P5 to P8).

Profile	P5	P6	P7A	P7B	P8A	P8B
QWINDS	$1.10 \times 10^{-7}$	$9.00 \times 10^{-8}$	$9.20 \times 10^{-8}$	$9.20 \times 10^{-8}$	$9.00 \times 10^{-7}$	I. $9.30 \times 10^{-8}$ II. $3.00 \times 10^{-7}$
CIMPACT	$1.00 \times 10^{-5}$	I. $1.00 \times 10^{-6}$ II. $1.00 \times 10^{-5}$				
AR	$2.00 \times 10^{-7}$	$2.75 \times 10^{-6}$	$1.10 \times 10^{-5}$	$4.40 \times 10^{-6}$	$-5.00 \times 10^{-6}$	I. $-5.00 \times 10^{-6}$ II. $2.00 \times 10^{-6}$

The evolution of  $Y_B$  for all the profiles of the Sand Motor study area is represented in Figure 11, and values of  $Y_S$  are presented in Figure 12.

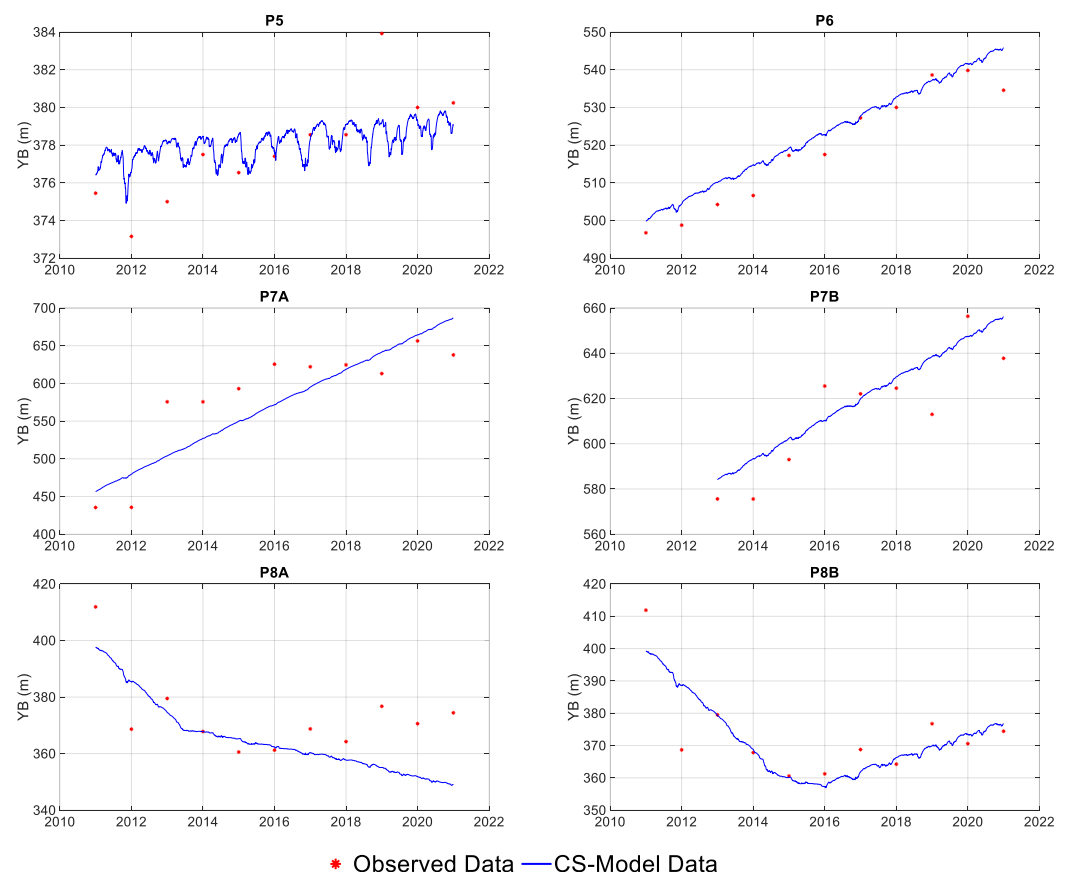


**Figure 11.** Evolution of modeled (blue) and observed (red) values of berm position ( $Y_B$ ).

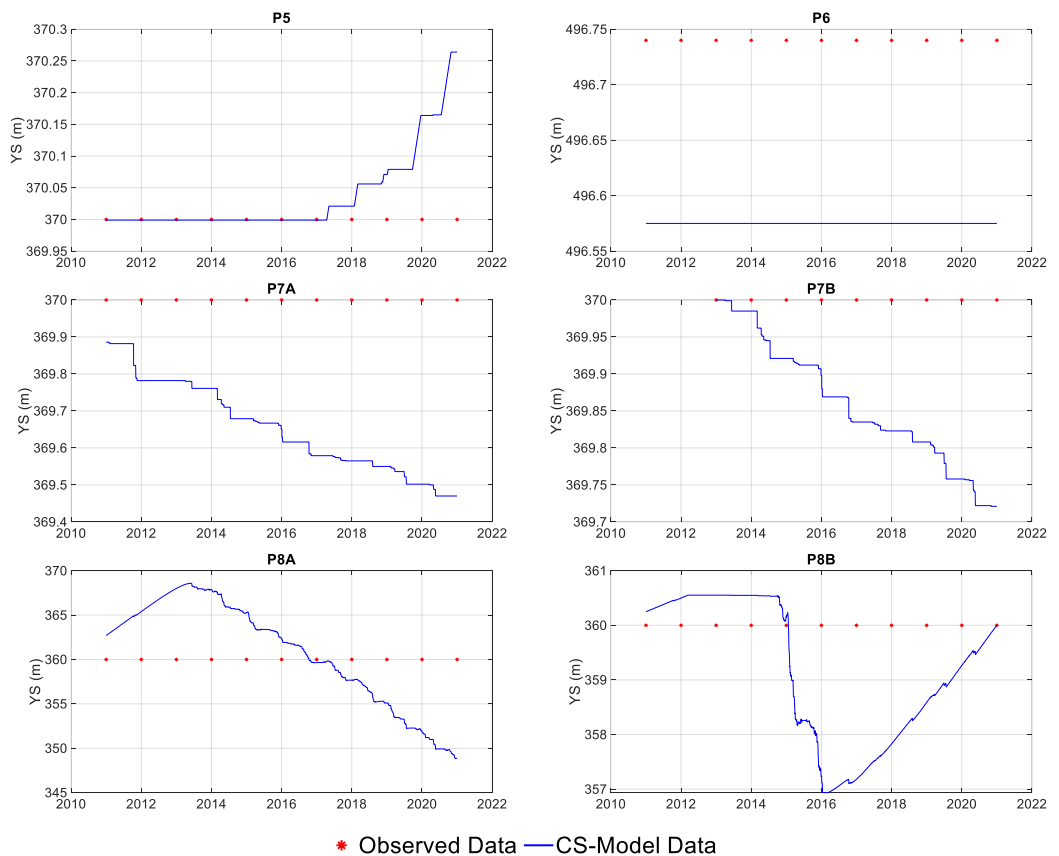


**Figure 12.** Evolution of modeled seaward dune foot position (blue) and observed values of seaward dune foot position (red).

Table 11 summarizes the mean absolute error of  $Y_B$  and  $Y_S$  for each profile. In profile P5, the simulated values of  $Y_S$  were close to the observed values, with a mean absolute error of 0.03 m and a maximum difference of about 0.27 m in 2021. Similar conclusions can be reached for the P6 profile, where there was a constant difference of 0.17 m throughout the entire simulation. For the P7A approach, the mean absolute error was 0.33 m, but it improved to 0.12 m when the first two years were ignored (P7B). Finally, for the P8A simulation, the mean absolute error was 4.68 m, but when the simulations were divided into two periods, the mean absolute error was 1.23 m (P8B). For  $Y_B$  in the P5 profile, the simulated results compare well with the observed values, with a mean absolute error of 1.64 m. The same conclusions can be drawn from the P6 profile, although with a higher mean absolute error (3.53 m). Profile P7A had the highest  $Y_B$  mean absolute error (38.22 m), but when the first two years were ignored, the results improved and the mean absolute error decreased to 11.37 m. Finally, for profile P8, simulations with the P8A sets had a mean absolute error of 10.20 m. When the two parts were simulated separately (P8B), the mean absolute error decreased to 5.60 m. The results of mean absolute error for P8B show good comparison between simulated values and observed values of  $Y_B$ .

**Table 11.** Mean absolute error of  $Y_B$  and  $Y_S$  for each profile at the Sand Motor study area applying EUR wave climate dataset.

Mean Absolute Error (m)	P5	P6	P7A	P7B	P8A	P8B
$Y_B$	1.64	3.53	38.22	11.37	10.20	5.60
$Y_S$	0.03	0.17	0.33	0.12	4.68	1.23

#### 4.4. Remarks

In this section, several different analyses are presented, allowing for a richer discussion of the main conclusions. First, the mean mobile average error is estimated for the  $Y_B$  and  $Y_S$  parameters, at both the IJmuiden and Sand Motor study areas (Figure 13). The mobile period considered for IJmuiden was 10 years and that for Sand Motor, 3 years. This analysis allows for verification that there were no increasing errors over the period of simulation.

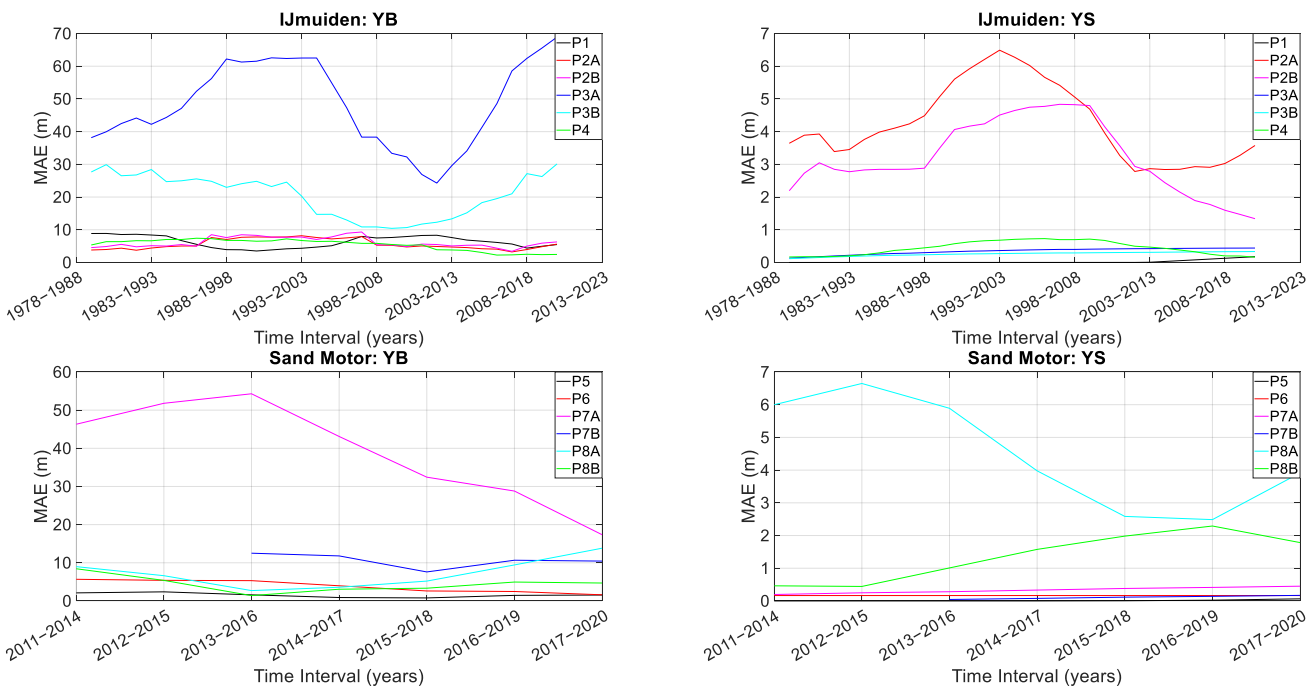


**Figure 13.** Mean mobile average error for  $Y_B$  and  $Y_S$  parameters at IJmuiden (10 year average intervals) and Sand Motor (3 year average intervals) study areas.

The mean mobile average error can represent fluctuations using the CS-Model. For the IJmuiden study area, the  $Y_B$  values for P1, P2, and P4 locations are similar, while P3 fluctuates between 10 and 65 m error. As previously mentioned, profile P3 is located in the proximity of the south groin and different trends are observed there, making it difficult to simulate the observed behavior. First, an important accumulation of sand is registered and so an advancement of the berm position to offshore should be represented. Later, a near-equilibrium situation is established, decreasing the moving rate of the berm. In the same way, the  $Y_S$  error values for P3 show more fluctuations ranging between 1 and 6.5 m. For the Sand Motor study area, the  $Y_S$  position errors of P7 differ from the other profiles' behavior, most likely due to the distance and location of this profile from the construction site and consequent erosion and accretion patterns observed south of Sand Motor due to longshore sediment transport processes (diffusion of sand and groin effects of the nourishment). The  $Y_S$  values of profile P8 show 3-year MAE fluctuations ranging from 0.5 to 6.5 m, which relates to natural erosion in the first years after construction of the mega-nourishment and subsequent groin effects (some sediments can be trapped by Sand Motor).

Additional tests considered the  $Y_B$  calibration for profile P1 at IJmuiden. Analysis of the first 6 and 10 years used for calibration showed that those years are far from being well represented by the model (Figure 14). When considering different time ranges of data for calibration (5, 10, 15, 20, 25, 30 and 35 years of the 1979–2020 period were evaluated), different accretion rates are considered, and therefore, the mean absolute error for the considered time interval also changes. In Table 12, an analysis of the model calibration considering different time ranges for profile P1 is obtained.

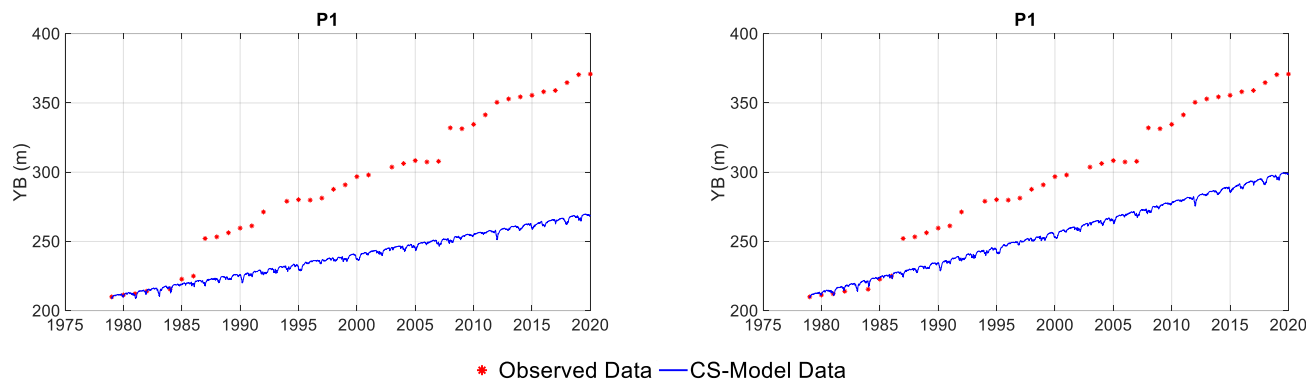


**Figure 14.** Calibration of  $Y_B$  (m) using first 6 years (**left**) and 10 years (**right**) at the P1 profile with the remaining years used for model validation.

**Table 12.** Mean absolute error of  $Y_B$  and  $Y_S$  for profile P1 considering different time ranges and accretion rates.

Calibration Period (Years)	Mean Absolute Error: $Y_B$ (m)	Mean Absolute Error: $Y_S$ (m)	AR (m/Time Step)
2015–2020	1.89	0.002	$2.1 \times 10^{-6}$
2010–2020	2.88	0.185	$2.3 \times 10^{-6}$
2005–2020	4.63	0.111	$2.7 \times 10^{-6}$
2000–2020	4.49	0.088	$2.3 \times 10^{-6}$
1995–2020	4.89	0.071	$2.2 \times 10^{-6}$
1990–2020	4.23	0.062	$2.3 \times 10^{-6}$
1985–2020	6.77	0.052	$2.7 \times 10^{-6}$
1979–2020	5.39	0.045	$2.4 \times 10^{-6}$

As Figure 14 shows, for extended periods of data, it is difficult to identify trends correctly. If a 6-year time series and profile data (five surveys) are used to calibrate P1, an AR equal to  $9.00 \times 10^{-7}$  m/time step (0.26 cm/year) is obtained. Therefore, the mean absolute error of  $Y_B$  could be reduced to 1.47 m, comparing simulated and observed data. However, simulations of the following years would increase the mean absolute error to 54.76 m. Calibration of the P1 profile considering the first 10 years of data would result in a mean absolute error of 6.52 m, altering the AR to  $1.30 \times 10^{-6}$  m/time step (0.38 cm/year). However, the following years' simulations would present a mean absolute error of 39.74 m.

Table 12 allows for discussion of the impact of choosing an adequate period of analysis for CS-Model simulations.

In general, calibration of the  $Y_B$  parameter is better when fewer years are used (minor values of mean absolute errors) as it is easier to represent shorter periods of data. However, the significance of trends is not as well represented in short calibration runs.  $Y_S$  is less sensitive to the period of data considered in the simulations as it is also moving less.

Finally, because of the uncertainties related to the high dynamics after the first years of construction of Sand Motor, additional simulations for profiles P5 to P8 were performed considering the time period after 2014. The mean absolute error of dune foot and berm positions was evaluated considering new input parameters (Table 13). Figures 15 and 16 show the results of the berm and the dune toe position evolution, respectively.

**Table 13.** Adopted QWINDS ( $\text{m}^3/\text{s}/\text{m}$ ), CIMPACT and accretion rate (AR,  $\text{m}/\text{time step}$ ) in CS-Model for each profile.

Profile	P5	P6	P7	P8
QWINDS	$1.00 \times 10^{-7}$	$9.00 \times 10^{-8}$	$9.20 \times 10^{-8}$	$1.50 \times 10^{-7}$
CIMPACT	$1.00 \times 10^{-5}$	$1.00 \times 10^{-5}$	$1.00 \times 10^{-5}$	$1.00 \times 10^{-5}$
AR	$2.00 \times 10^{-7}$	$3.40 \times 10^{-6}$	$4.00 \times 10^{-6}$	$1.00 \times 10^{-6}$

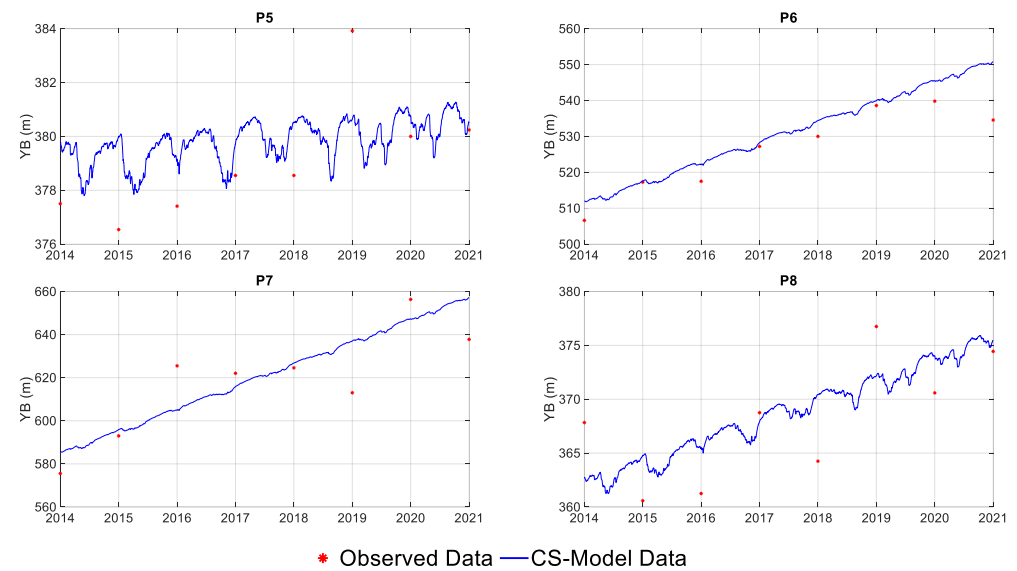


**Figure 15.** Evolution of modeled (blue) and observed (red) values of berm position ( $Y_B$ ) for Sand Motor between 2014 and 2021.

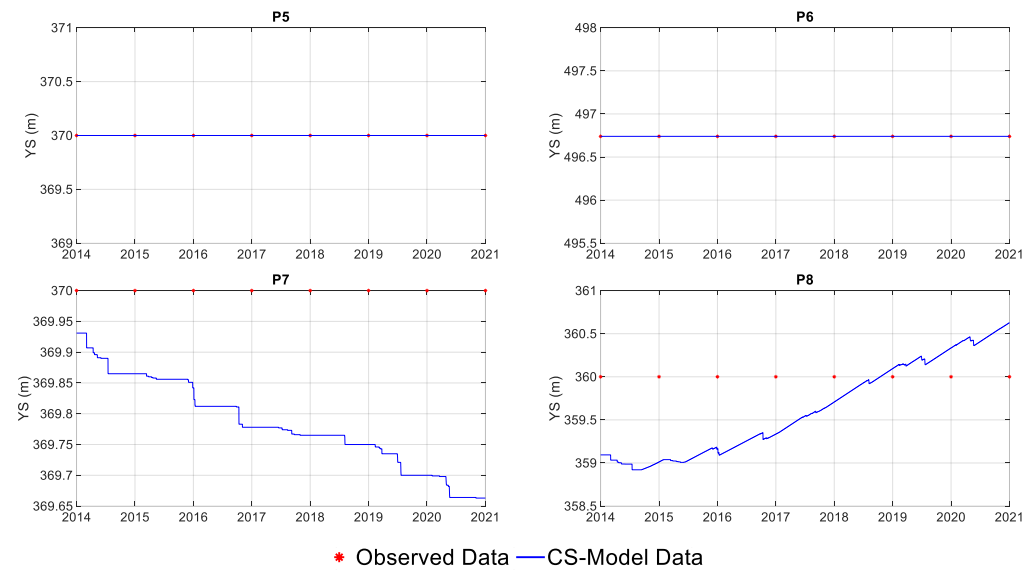


**Figure 16.** Evolution of modeled (blue) and observed (red) values of seaward dune foot position ( $Y_S$ ) for Sand Motor between 2014 and 2021.

Considering the new simulations, the values of mean absolute error are presented in Table 14.

**Table 14.** Mean absolute error of  $Y_B$  and  $Y_S$  for each profile applying the EUR wave climate dataset at Sand Motor study area for the period 2014–2021.

Mean Absolute Error (m)	P5	P6	P7	P8
$Y_B$	2.00	3.15	11.55	3.34
$Y_S$	0.00	0.00	0.20	0.58

The simulated values of  $Y_B$  show good agreement (better than for the period 2011–2021) with observations (values of mean absolute error less than 3.34 m) with the exception of profile P7. This profile was previously evaluated by dividing the calibration into two periods, and a value of the same order of magnitude was found (P7B, in Table 11).  $Y_S$  shows a better agreement between observed and simulated values, with a MAE of less than or equal to 0.58 m for all profiles considered.

## 5. Discussion Dataset Extension

It is interesting to note that the calibration of the CS-Model with over 40 years of data in the IJmuiden case did not lead to an overall better performance of the model than with calibration with 10 years of data in the Sand Motor case. Calibration with a relatively long time series captures the overall trend of the beach evolution, and therefore, the longer the scale is, the more smoothed out individual events become. Calibration with a longer time series is not applicable if the conditions change, as is the case in the evolution of profiles P3 and P8.

For P3, the mean absolute error of  $Y_B$  reduced from 49.75 to 23.30 m when considering two smaller periods of the extensive dataset for the IJmuiden study area, each covering the two apparent phases of the evolution. For the P8A and P8B profiles of the Sand Motor study area, the mean absolute error of  $Y_B$  was reduced from 10.20 m to 5.60 m by changing the input parameters and considering two smaller periods. For this location, errors may be related to the first year's dynamics after the construction of Sand Motor. This means that the CS-Model needs to be applied carefully in locations where significant anthropogenic actions (groins and nourishments in this study) occur.

In general, the CS-Model calibration performance improved when a 10-year simulation period was used in the Sand Motor study area instead of the 41-year simulation period at IJmuiden (lower mean absolute error). For the IJmuiden study area, considering fewer years of simulations (2015–2020) also led to better representation of the berm position evolution, as opposed to using a 41-year calibration period. For Sand Motor, starting simulations in 2014 led to better results than starting at 2011, which is just after the mega-nourishment construction.

CS-Model studies have considered a range of calibration periods. For example, Marinho et al. [15] used a 4-year calibration period and a model validation period of 4 years, using 8 years of profile and wave climate data to simulate two bar migrations. Another example can be found from Hallin et al. [30], who used a dataset of 22 years of morphologic and hydrologic data (1994–2016), with CS-Model simulations divided into two parts: the first part corresponding to the calibration of the model (1994–2010) and the second part corresponding to the validation of the model data (2010–2016). The results showed satisfactory capability to hindcast the beach and dune evolution in the study area [30]. Therefore, the CS-Model needs to be applied carefully in future projections if the objective is to perform long-term simulations supported by long datasets of profile and wave climate where profile variations are observed over time. If a future medium-term (5–10 years) projection is intended, then less information is needed to calibrate the model.

Other authors have applied the CS-Model with different objectives, considering fewer years for calibration purposes and using shorter datasets of measured profiles. Their conclusions were that the CS-Model can be used to study different behaviors in cross-shore profiles (namely the berm position evolution and dune changes), but morphological changes were not quantified in their works ( $Y_B$  and  $Y_S$  changes). Table 15 shows the number

of profiles and surveys and the extent of data used to calibrate the CS-Model in several other studies.

**Table 15.** Number of profiles and time period considered to calibrate the CS-Model.

Author	Study Area	Number of Profiles	Number of Surveys	Years for Calibration
Marinho [47]	Costa-Nova, Portugal	1	6	4
	Duck, NC, USA	1	~144	4
	Silver Strand, CA, USA	1	9	2
	Cocoa Beach, FL, USA	2	5	1
Hallin et al. [30]	South IJmuiden, The Netherlands	26	4	16
Palalane et al. [9]	Costa-Nova, Portugal	1	6	4
	Macaneta spit, Mozambique	2	1–2	18
	Ängelholm, Sweden	3	17	19.5
This work	IJmuiden, The Netherlands	4	41	41
	Sand Motor, The Netherlands	4	10	10

Marinho [47] simulated a one-year artificial nourishment evolution from June 1992 to July 1993, performed at Cocoa Beach, Florida, USA. Simulations using the CS-Model were judged “good” considering the transference of material towards the shore and evolution of nourishment in agreement with observations. Hallin et al. [30] used 16 years of wave climate data (from 1994 to 2010) and four profiles (spacing every 5 years, between 1995 and 2010) in 26 alongshore locations to calibrate the CS-Model. The objective of the work was to investigate the impact of beach sediment supply on dune volume evolution in south IJmuiden (Kennemer dunes) in the Netherlands. The simulated evolution of the dune system was in good agreement with observed data, proving that the CS-Model has a satisfactory capability to hindcast dune evolution in a fast and stable way. Palalane et al. [9] applied the CS-Model to study the evolution of a beach–dune system on a decadal scale. In this work, 17 profiles were used to calibrate for 19.5 years (between 1995 to 2014) at three locations in Ängelholm, Sweden. The model was successfully applied in the study area and the results show good agreement between observed and simulated data. A high number of profiles used to calibrate the CS-Model was considered by Marinho [47]. Data acquisition occurred 2–3 times per month between January 1981 and December 1989 at Duck, North Carolina, USA. The model was applied to evaluate the volume of individual bars (inner and outer bar) within the time period of analysis. The simulated results agreed with the observed evolution in the study area.

## 6. Conclusions

Numerical models are used to represent real processes but require calibration for adequate characterization of a specific parameter. In this case, the CS-Model was used to represent the evolution of cross-shore profiles at IJmuiden and Sand Motor in the Netherlands. A total of four profiles were considered at each site. The parameter chosen to calibrate the model was the berm position, which moves in an offshore direction over time in most of the adopted profiles (P1 and P3 to P8). In P2, however, the berm position retreats with time. The CS-Model considers the mass balance, which means that changes between the dune and berm and the berm and bar do not add/remove mass to/from the system. As the considered profiles have erosion/accretion trends, a shoreline position variation rate was considered, making it difficult to represent specific variations observed over time.

The obtained results show the simulated evolution of the berm position. Profile P3 has a major mean absolute error (49.75 m), but if the simulation is divided in two periods with different accretion rates, the mean absolute error is reduced (23.30 m). When datasets

derived from global models (three different ones) were considered for wave climate, the results of  $Y_B$  and  $Y_S$  simulations did not show significative changes (same magnitude of values for each profile). For instance, the P1 profile had a mean absolute error of berm position ( $Y_B$ ) of 5.39 m for the YM6 dataset, 5.79 m for the ERA5 dataset, 5.87 m for the AENWS-WPR dataset and 5.84 m for the AENWS-WPR-Shore dataset. The ERA5 dataset was expected to have the lowest quality, and it did, but it still did not have significantly larger errors than the measurement data (YM6).

After comparison with several different published studies, it was realized that the CS-Model performs best when calibration data extend for 5 to 10 years. Projections should also consider this time period. The results from the current study show that better results were achieved when a 10-year calibration period was used for the Sand Motor study area compared to a 40-year calibration period for IJmuiden. Model calibration with such extensive datasets is not common, and this work presents the results of a long-term calibration period resulting in an evaluation of CS-Model performance. The calibration process of the CS-Model with extensive observed datasets from the IJmuiden area shows the importance of main trends with time. Considering long-term datasets of wave climate and profile data, accretion/erosion trends can be identified, including the contribution from the effects of coastal defense measures such as artificial nourishments that change the longshore sediment transport conditions with time. Numerical modeling of beach profiles in medium-to long-term perspectives can help managers define better solutions to mitigate coastal erosion. However, uncertainties in modeling future conditions will continue to exist, as anticipating wave climates and data for calibration requires interpretation and adequate forecasting. It is important to interpret beach profile behavior properly, keeping in mind that modeling results are dependent on inputs and calibration assumptions. However, if adequate calibration is performed, cross-shore numerical models can serve as an important tool to support coastal management decisions regarding, for instance, artificial nourishment interventions.

As mentioned above, this work was developed as part of the AX-COAST project, and therefore, the IJmuiden study area was chosen to apply the new tool, taking advantage of long physical and morphological datasets. The next step is to apply the calibrated model with future wave conditions and evaluate the influence of different strategies of coastal defense (especially artificial nourishments) considering different volumes, frequencies of nourishments and deposition locations in the cross-shore profile and considering a time range of 5–10 years.

**Author Contributions:** Conceptualization, F.R. and H.Á.; methodology, F.R. and H.Á.; software, F.R.; validation, F.R., C.C. and M.L.; formal analysis, F.R.; investigation, F.R.; resources, H.Á. and E.M.M.; data curation, F.R., H.Á. and E.M.M.; writing—original draft preparation, F.R.; writing—review and editing, C.C., M.L., H.Á. and E.M.M.; visualization, C.C., M.L., H.Á. and E.M.M.; supervision, C.C.; project administration, C.C. and M.L.; funding acquisition, C.C. and M.L. All authors have read and agreed to the published version of the manuscript.

**Funding:** This work was financially supported by the AX-COAST project: Cross-shore features and internationalization of the COAST, funded by the EEA Grants within the scope of the Blue Growth program, managed by the Direção-Geral de Política do Mar. The work received financial support from A-AAGORA innovation action co-funded by the European Union under the Horizon Europe Program, Grant No. 101093956.

**Institutional Review Board Statement:** Not applicable.

**Informed Consent Statement:** Not applicable.

**Data Availability Statement:** No new data were created or analyzed in this study. Data sharing is not applicable to this article.

**Acknowledgments:** The authors would like to thank to A-AAGORA project to allow the publication of this article.

**Conflicts of Interest:** The authors declare no conflict of interest.

## References

- Coelho, C.; Lima, M.; Ferreira, M. A Cost–Benefit Approach to Discuss Artificial Nourishments to Mitigate Coastal Erosion. *J. Mar. Sci. Eng.* **2022**, *10*, 1906. [[CrossRef](#)]
- Ferreira, A.M.; Coelho, C. Artificial nourishments effects on longshore sediments transport. *J. Mar. Sci. Eng.* **2021**, *9*, 240. [[CrossRef](#)]
- Lima, M. Ferramenta Numérica de Análise do Impacto de Intervenções de Defesa Costeira na Evolução da Linha de Costa: Custos e Benefícios. Ph.D. Thesis, University of Aveiro, Aveiro, Portugal, 2018; p. 336.
- Coelho, C. Riscos de Exposição de Frentes Urbanas para Diferentes Intervenções de Defesa Costeira. Ph.D. Thesis, University of Aveiro, Aveiro, Portugal, 2005; p. 404.
- Lima, M.; Coelho, C. O modelo de evolução da linha de costa LTC: Pressupostos, evolução, validação e aplicação. *Rev. De Gestão Costeira Integr.* **2017**, *17*, 5–17. [[CrossRef](#)]
- Lima, M. Programação de Métodos de Pré-Dimensionamento de Obras Costeiras. Master’s Thesis, University of Aveiro, Aveiro, Portugal, 2011; p. 166.
- Lima, M.; Coelho, C.B.; Cachim, P.B. Programming methods for pre-design of coastal structures. In Proceedings of the V International Conference on Computational Methods in Marine Engineering (MARINE 2013), Hamburg, Germany, 29–31 May 2013; pp. 868–879. Available online: <https://www.aprh.pt/raci/raci-n44.html> (accessed on 12 March 2024).
- Davidson, M.A.; Splinter, K.D.; Turner, I.L. A simple equilibrium model for predicting shoreline change. *Coast. Eng.* **2013**, *73*, 191–202. [[CrossRef](#)]
- Palalane, J.; Fredriksson, C.; Marinho, B.; Larson, M.; Hanson, H.; Coelho, C. Simulating cross-shore material exchange at decadal scale. Model application. *Coast. Eng.* **2016**, *116*, 26–41. [[CrossRef](#)]
- Robinet, A.; Idier, D.; Castelle, B.; Marieu, V. A reduced complexity shoreline change model combining longshore and cross shore processes: The LX-Shore model. *Environ. Model. Softw.* **2018**, *109*, 16. [[CrossRef](#)]
- Roelvink, J.A.; Reniers, A.; van Dongeren, A.R.; van Thiel de Vries, J.S.M.; McCall, R.; Lescinski, J. Modeling storm impacts on beaches, dunes and barrier islands. *Coast. Eng.* **2009**, *56*, 1133–1152. [[CrossRef](#)]
- Larson, M.; Kraus, N.C. *SBEACH: Numerical Model for Simulating Storm-Induced Beach Change, Report 1: Empirical Foundation and Model Development*; U.S. Army Engineer Waterways Experiment Station, Coastal Engineering Research Center: Vicksburg, MS, USA, 1989.
- DHI. *DHI-Profile Development, LITPROF User Guide*; Danish Hydraulic Institute: Hørsholm, Denmark, 2008.
- Ruessink, B.G.; Kuriyama, Y.; Reniers, A.J.H.M.; Roelvink, J.A.; Walstra, D.J.R. Modeling cross-shore sandbar behavior on the timescale of weeks. *J. Geophys. Res. Earth Surf.* **2007**, *112*, 1–15. [[CrossRef](#)]
- Marinho, B.; Coelho, C.; Larson, M.; Hanson, H. Cross-shore modelling of multiple nearshore bars at a decadal scale. *Coast. Eng.* **2020**, *159*, 103722. [[CrossRef](#)]
- Larson, M.; Palalane, J.; Fredriksson, C.; Hanson, H. Simulating cross-shore material exchange at decadal scale. Theory and model component validation. *Coast. Eng.* **2016**, *116*, 57–66. [[CrossRef](#)]
- Hanson, H.; Kraus, N. *GENESIS—Generalised Model for Simulating Shoreline Change; Report TR-CERC 89-19 (Report 1)*; Coastal and Hydraulic Laboratory, US Army Corps of Engineers: Washington, DC, USA, 1989.
- Hanson, H. GENESIS: A generalized shoreline change numerical model. *J. Coast. Res.* **1989**, *5*, 1–27. Available online: <http://www.jstor.org/stable/4297483> (accessed on 12 March 2024).
- Delft3D Website. Deltares, NL. Available online: <https://oss.deltares.nl/web/delft3d> (accessed on 15 April 2024).
- Xu, Z.; Plink-Björklund, P. Quantifying Formative Processes in River- and Tide-Dominated Deltas for Accurate Prediction of Future Change. *Geophys. Res. Lett.* **2023**, *50*, e2023GL104434. [[CrossRef](#)]
- Larson, M.; Kraus, N.C.; Hanson, H. Simulation of regional longshore sediment transport and coastal evolution—The “CASCADE” model. *Coast. Eng.* **2002**, *2002*, 2612–2624.
- Bizzi, S.; Tangi, M.; Schmitt RJ, P.; Pitlick, J.; Piégay, H.; Castelletti, A.F. Sediment transport at the network scale and its link to channel morphology in the braided Vjosa River system. *Earth Surf. Process. Landf.* **2021**, *46*, 2946–2962. [[CrossRef](#)]
- Dabees, M.; Kamphuis, J.W. ONELINE, a numerical model for shoreline change. *Coast. Eng.* **1998**, *1999*, 2668–2681. [[CrossRef](#)]
- Hamza, W.; Tomasicchio, G.R.; Ligorio, F.; Lusito, L.; Francone, A. A Nourishment Performance Index for Beach Erosion/Accretion at Saadiyat Island in Abu Dhabi. *J. Mar. Sci. Eng.* **2019**, *7*, 173. [[CrossRef](#)]
- Francone, A.; Simmonds, D.J. Assessing the Reliability of a New One-Line Model for Predicting Shoreline Evolution with Impoundment Field Experiment Data. *J. Mar. Sci. Eng.* **2023**, *11*, 1037. [[CrossRef](#)]
- Kalligeris, N.; Smit, P.B.; Ludka, B.C.; Guza, R.T.; Gallien, T.W. Calibration and assessment of process-based numerical models for beach profile evolution in southern California. *Coast. Eng.* **2020**, *158*, 103650. [[CrossRef](#)]
- Simmons, J.A.; Splinter, K.D.; Harley, M.D.; Turner, I.L. Calibration data requirements for modelling subaerial beach storm erosion. *Coast. Eng.* **2019**, *152*, 103507. [[CrossRef](#)]
- Paravath, K.; Thuvanasmal, N. Shoreline Changes Around Three Estuarine Harbours on Kerala Coast in India. *Int. J. Civ. Eng.* **2023**, *10*, 29–44. [[CrossRef](#)]
- Monecke, K.; Meilianda, E.; Walstra, D.-J.; Hill, E.M.; McAdoo, B.G.; Qiu, Q.; Storms JE, A.; Masputri, A.S.; Mayasari, C.D.; Nasir, M.; et al. Postseismic coastal development in Aceh, Indonesia—Field observations and numerical modeling. *Mar. Geol.* **2017**, *392*, 94–104. [[CrossRef](#)]

30. Hallin, C.; Huisman BJ, A.; Larson, M.; Walstra, D.-J.R.; Hanson, H. Impact of sediment supply on decadal-scale dune evolution—Analysis and modelling of the Kennemer dunes in the Netherlands. *Geomorphology* **2019**, *337*, 94–110. [[CrossRef](#)]
31. Ministerie van Verkeer en Waterstaat. *3e Kustnota, Traditie, Trends en Toekomst*; Ministerie van Verkeer en Waterstaat: Amsterdam, The Netherlands, 2000; p. 124.
32. Brand, E.; Ramaekers, G.; Lodder, Q. Dutch experience with sand nourishments for dynamic coastline conservation—An operational overview. *Ocean. Coast. Manag.* **2022**, *217*, 106008. [[CrossRef](#)]
33. Rijkswaterstaat, Ministerie van Infrastructuur and Waterstaat. Available online: <https://www.rijkswaterstaat.nl/> (accessed on 21 March 2024).
34. Li, F.; van Gelder PH AJ, M.; Ranasinghe, R.; Callaghan, D.P.; Jongejan, R.B. Probabilistic modelling of extreme storms along the Dutch coast. *Coast. Eng.* **2014**, *86*, 1–13. [[CrossRef](#)]
35. Van Rijn, L. Improvement of Coastline Modelling Software Using Field Data. AX-COAST Report (non published). 2023.
36. METAR & TAF, Visual Decoder. Available online: <https://metar-taf.com/> (accessed on 21 March 2024).
37. Herman PM, J.; Moons JJ, S.; Wijsman JW, M.; Luijendijk, A.P.; Ysebaert, T. A Mega-Nourishment (Sand Motor) Affects Landscape Diversity of Subtidal Benthic Fauna. *Front. Mar. Sci.* **2021**, *8*, 643674. [[CrossRef](#)]
38. Wijnberg, K.M. Environmental controls on decadal morphologic behaviour of the Holland coast. *Mar. Geol.* **2002**, *189*, 227–247. [[CrossRef](#)]
39. Stronkhorst, J.; Huisman, B.; Giardino, A.; Santinelli, G.; Santos, F.D. Sand nourishment strategies to mitigate coastal erosion and sea level rise at the coasts of Holland (The Netherlands) and Aveiro (Portugal) in the 21st century. *Ocean. Coast. Manag.* **2018**, *156*, 266–276. [[CrossRef](#)]
40. Vermas, T.; Boersen, S.; Wilmink, R.; Lodder, Q. *National Analyses of Nourishments; Coastal State Indicators and Driving Forces for Bergen-Egmond, The Netherlands*; Rijkswaterstaat and Deltares: Delft, The Netherlands, 2021.
41. Huisman, B.J.A.; Ruessink, B.G.; de Schipper, M.A.; Luijendijk, A.P.; Stive, M.J.F. Modelling of bed sediment composition changes at the lower shoreface of the Sand Motor. *Coast. Eng.* **2018**, *132*, 33–49. [[CrossRef](#)]
42. Wijsman, J.W.M.; Craeymeersch, J.A.; Herman, P.M.J. Comparing grab and dredge sampling for shoreface benthos using ten years of monitoring data from the Sand Motor mega nourishment. *J. Sea Res.* **2022**, *188*, 102259. [[CrossRef](#)]
43. Hersbach, H.; Bell, B.; Berrisford, P.; Biavati, G.; Horányi, A.; Muñoz Sabater, J.; Nicolas, J.; Peubey, C.; Radu, R.; Rozum, I.; et al. ERA5 Hourly Data on Single Levels from 1940 to Present. Copernicus Climate Change Service (C3S) Climate Data Store (CDS). 2023. Available online: <https://cds.climate.copernicus.eu/cdsapp#!/dataset/10.24381/cds.adbb2d47> (accessed on 31 November 2023).
44. Atlantic-European North West Shelf-Wave Physics Reanalysis. E.U. Copernicus Marine Service Information (CMEMS). Marine Data Store (MDS). Available online: [https://data.marine.copernicus.eu/product/NWSHELF\\_REANALYSIS\\_WAV\\_004\\_015\(description](https://data.marine.copernicus.eu/product/NWSHELF_REANALYSIS_WAV_004_015(description)) (accessed on 31 November 2023).
45. Ásmundsson, H. Sensitivity analysis of global datasets at IJmuiden. Validation of wave climate data. MEMO of the AX-Coast project (non published). 2024.
46. Guillén, J.; Stive, M.J.F.; Capobianco, M. Shoreline evolution of the Holland coast on a decadal scale. *Earth Surf. Process. Landf.* **1999**, *24*, 517–536. [[CrossRef](#)]
47. Marinho, B. Alimentações Artificiais Como Solução de Defesa Costeira: Abordagens de Monitorização e Modelação. Ph.D. Thesis, University of Aveiro, Aveiro, Portugal, 2018; p. 359.

**Disclaimer/Publisher’s Note:** The statements, opinions and data contained in all publications are solely those of the individual author(s) and contributor(s) and not of MDPI and/or the editor(s). MDPI and/or the editor(s) disclaim responsibility for any injury to people or property resulting from any ideas, methods, instructions or products referred to in the content.